The Australian Landscape Water Balance model (AWRA-L v6)

Technical Description of the Australian Water Resources Assessment Landscape model version 6

Version number/type	Date of issue
3.0	30/11/2018

Contact details

Dr. Andrew Frost

Senior Hydrologist, Water Resources Modelling Unit

Bureau of Meteorology
PO Box 413, Darlinghurst NSW 1300

Tel: +61 2 9296 1517
Email: Andrew.Frost@bom.gov.au

Dr. Chantal Donnelly

Unit Head, Water Resources Modelling Unit

Bureau of Meteorology
GPO Box 413 Brisbane QLD 4001

Tel: +61 7 3239 8767
Email: Chantal.Donnelly@bom.gov.au

AWRA Modelling Team:

Water Resources Modelling Unit, Water Program

Email: awrams@bom.gov.au

Summary

This technical report provides a detailed description of the Bureau of Meteorology's operational Australian Water Resources Assessment Landscape model: AWRA-L version 6. The report includes a description of:

- the overall conceptual structure
- the model components (water balance, atmospheric vapour fluxes, energy balance, and vegetation phenology), and
- how the model was parameterised nationally

Process equations are provided along with a brief background on their choice and individual parameterisation.

The parameterisation described is as used to produce outputs on the operational Australian Landscape Water Balance website www.bom.gov.au/water/landscape.

Coding references are as implemented in the Bureau of Meteorology's AWRA Community Modelling system (https://github.com/awracms/awra_cms).

The model performance against observations and benchmarking against other models is summarised in a companion report (see Frost and Wright, 2018a; the AWRA-L v6 model evaluation report).

A reference guide for parameters used in the model code and within this document is provided in Appendix A.

Table of Contents

List of Tables

List of Figures

List of Acronyms

AVHRR:	Advanced Very High Resolution radiometer
AMSR-E:	Advanced Microwave Scanning Radiometer for the Earth Observing System
ASRIS:	Australian Soil Resource Information System
AWAP:	Australian Water Availability Project
AWRA-L:	Australian Water Resources Assessment Landscape Model
AWRA-R:	Australian Water Resources Assessment River Model
AWRAMS:	Australian Water Resource Assessment modelling system
BoM:	Bureau of Meteorology
CMRSET:	CSIRO MODIS reflectance-based Scaling ET
CSIRO:	Commonwealth Scientific and Industrial Research Organisation
ET:	Evapotranspiration
fPAR:	fraction of Photosynthetically Active Radiation absorbed by vegetation
HRU:	Hydrological Response Unit
LAI:	Leaf Area Index
NWA:	National Water Account
MODIS:	Moderate Resolution Imaging Spectroradiometer
RWI:	Regional Water Information
WIA:	Water in Australia
WIRADA:	Water Information Research and Development Alliance

1   Introduction

Prolonged extreme drought and resulting water shortages within Australia during the 'Millennium drought', over the period 1997 to 2009, triggered the implementation of the federally mandated Water Act (2007) towards better monitoring of water availability and water use nationwide. As a result, the Australian Bureau of Meteorology (the Bureau) was given responsibilities including collating water data from jurisdictional agencies and analysing and reporting on water status, in addition to its existing weather and flood forecasting responsibilities.

The Australian Water Resources Assessment (AWRA) Modelling System underpins the Bureau's water information services for national water resource assessment reporting, water use accounting and situation monitoring. The modelling system has been developed by the Bureau and CSIRO over the last decade and is run operationally at the Bureau to provide both situational awareness and national retrospective water resource assessment.

The AWRA-L (landscape) model runs on a daily timestep and 0.05° grid (approximately 5 km) simulating the landscape water balance for Australia from 1911 to yesterday. Key outputs from the AWRA-L model include surface runoff, soil moisture, evapotranspiration and deep drainage. Outputs from the model are available through the website interface (http://www.bom.gov.au/water/landscape); or on request as a registered user.

AWRA-L is optimised to the whole water balance using a national streamflow dataset along with satellite derived soil moisture and evapotranspiration estimates. The model is further validated against a wide range of observational datasets including point scale soil moisture probe data, flux tower estimates and groundwater recharge estimates (Frost and Wright, 2018a). The modelling system was released in 2016 as a community modelling system (https://github.com/awracms/awra_cms), enabling application and development by the wider research community.

Operational AWRA-L modelled outputs have been made publicly available since November 2015 (using AWRA-L version 5) and the modelled fluxes have been used internally and externally for various climatological, flood, water and agriculture applications across Australia. This document describes AWRA-L version 6 released operationally by the Bureau in late 2018.

1.1   The AWRA modelling system

The Australian Water Resources Assessment Modelling System (AWRAMS) underpins the Bureau water information services that are mandated through the Water Act (2007). The science of the AWRAMS (see Vaze *et al.*, 2013; Elmahdi *et al.*, 2015; Hafeez *et al.*, 2015); has been developed since July 2008 through the Water Information Research and Development Alliance (WIRADA) between CSIRO and the Bureau. The AWRAMS has been operational at the Bureau since 2011-12 for regular use in the National Water Account (NWA) and Water Resources Assessment reports. The

AWRAMS has evolved from AWRA v 0.5 (Van Dijk, 2010c) to AWRA v 5.0 (Viney *et al.*, 2015) and to AWRA v6.0 described here.

The operational AWRAMS simulates Australian landscape and river water stores and fluxes for the past 100+ years to now (Hafeez *et al.*, 2015). These estimates are updated on a daily basis and provide the current and historical context of water availability in Australia. Since the operational AWRA-L modelled outputs have been made publicly available in November 2015, the modelled fluxes have been used internally and externally for various climatological, flood, water and agriculture applications across Australia. The Bureau's AWRA team has been regularly interacting with a wide range of stakeholders about their needs and how these can be met by a daily operational water balance model. These interactions have spanned Commonwealth agencies and State government water and agriculture agencies, catchment management authorities, water utilities, consultants, water industry professionals, research organisations, universities and farmers.

This technical report describes the AWRA-L version 6.0 model structure and is intended to be used as a quick reference for the model equations and processes used in the Bureau's AWRA Community Modelling system. This document relies heavily on the following prior descriptions of AWRA-L:

- **AWRA-L v0.5**: Van Dijk, A. I. J. M. (2010c) *The Australian Water Resources Assessment System. Technical Report 3. Landscape Model (version 0.5) Technical Description*.
- **AWRA-L v5.0:** Viney, N., Vaze, J., Crosbie, R., Wang, B., Dawes, W. and Frost, A. (2015) *AWRA-L v5.0: technical description of model algorithms and inputs*. CSIRO, Australia.
- **AWRA-L v5.0:** Frost, A. J., Ramchurn, A., and Smith, A. (2016b). *The Bureau's Operational AWRA Landscape (AWRA-L) Model.* Bureau of Meteorology Technical Report.

Limited explanation is provided here for the derivation and choice of parameterisations. Van Dijk (2010c) provides the original design principles and the rationale for choice of the original national parametrisation in v0.5. Viney *et al.* (2015) describes the improvements that have been made in parameterisation and the conceptual structure of AWRA-L v5.0. This document updates the details of the model according to changes incorporated in AWRA-L v6.

1.2 Conceptual structure

AWRA-L (Van Dijk, 2010c; Viney *et al.*, 2014; Viney *et al.*, 2015; Frost *et al.*, 2016b) is a one dimensional, 0.05° grid based water balance model over the continent that has semi-distributed representation of the soil, groundwater and surface water stores. Within each grid cell there are three soil layers (top: 0-10cm, shallow: 10cm-100cm, deep: 100cm-600cm) and two hydrological response units (HRU: shallow rooted versus

deep rooted). Shallow rooted vegetation is assumed to have roots to the extent of the shallow soil layer (to 1m), while deep rooted vegetation is assumed to have roots down to 6 m (ie. the extent of the deep soil layer).

Key fluxes and stores output by AWRA-L as output of the operational Australian Landscape Water Balance website www.bom.gov.au/water/landscape include runoff, actual evapotranspiration, soil moisture for the three soil layers and deep drainage to the groundwater store - Figure 1. Note that different naming is used for the soil layers on the website and Figure 1 (Upper, Lower and Deep soil) than is used in this document (Top, Shallow and Deep soil). The naming used here is consistent with the code and previous documentation.
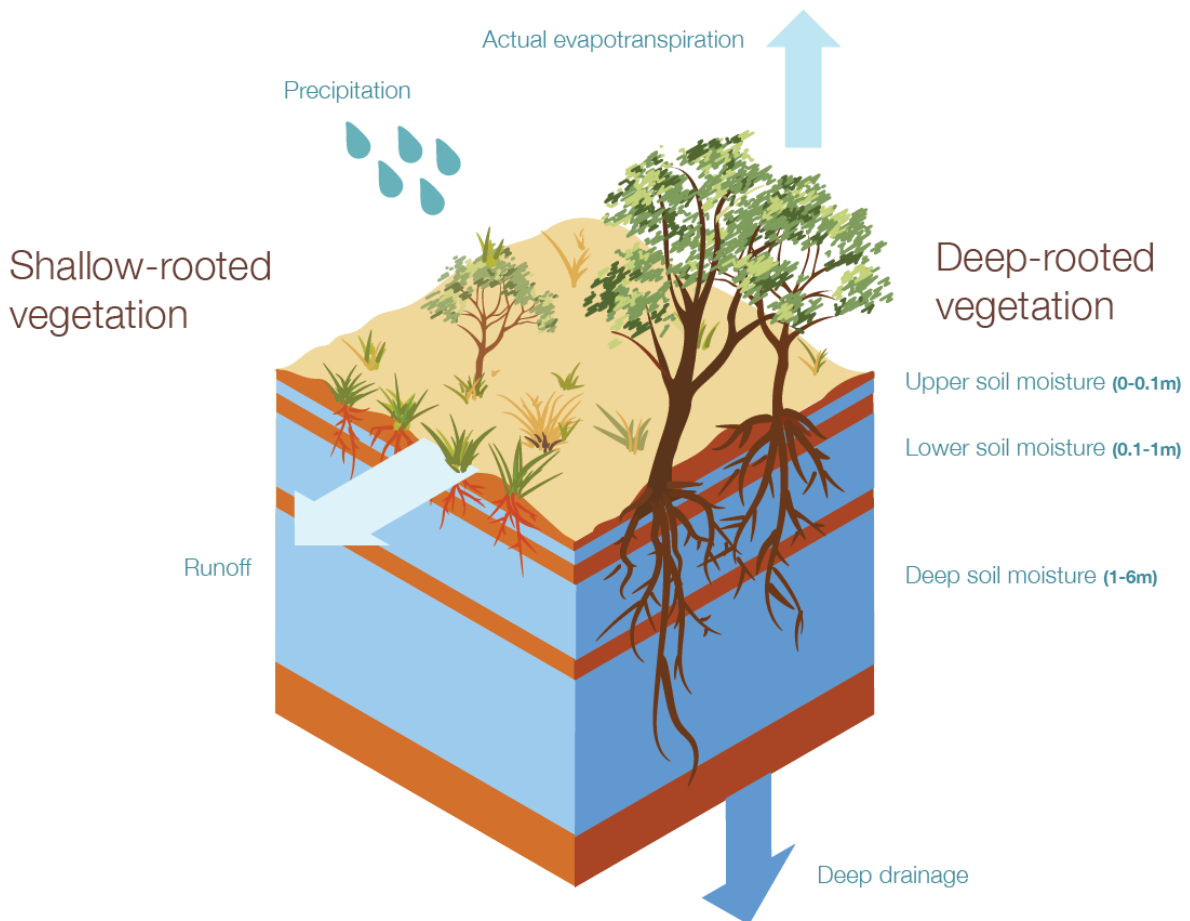
Figure 1. Conceptual AWRA-L grid cell with key water stores and fluxes shown

AWRA-L models hydrological processes for:

- Partitioning of rainfall between interception losses and net rainfall

- Saturation excess overland flow (depending on groundwater store saturation level)
- Infiltration and Hortonian (infiltration excess) overland flow
- Saturation, interflow, drainage and evaporation from soil layers
- Baseflow, evaporation and transpiration from the groundwater store

The soil layers are modelled separately for 2 (shallow and deep rooted) hydrological response units. In addition, the following vegetation processes are described:

- transpiration, as a function of maximum root water uptake and optimum transpiration rate;
- vegetation cover adjustment, as a function of the balance between the theoretical optimum and the actual transpiration, and at a rate corresponding to vegetation cover type.

The bottom levels of the top, shallow and deep soil layer within AWRA-L are chosen to be 0.1m, 1m and 6m respectively. Differing model parameters are chosen where appropriate for the shallow and deep rooted HRU's. Hydrologically, these two HRU's differ in their aerodynamic control of evaporation, in their interception capacities and in their degree of access to different soil layers. Groundwater and river water dynamics are simulated at grid cell level and hence parameters are uniform across the grid cell, and dynamic variables (e.g. fraction groundwater saturated area and open water within stream channels) are equal between HRUs.

Figure 2 shows the conceptual structure of the AWRA-L model (hereafter termed AWRA-L).
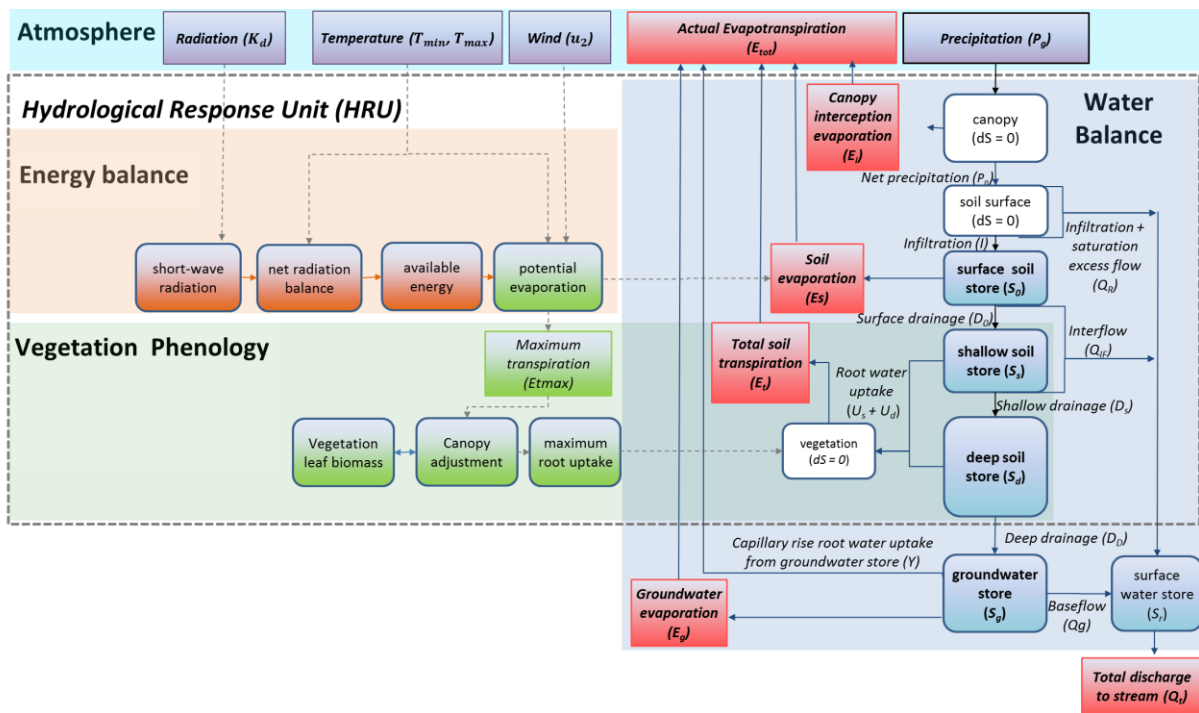
Figure 2. AWRA-L conceptual structure. Purple: climate inputs; Blue rounded boxes: water stores; Red boxes: water flux outputs; Brown: energy balance; Green rounded boxes: vegetation processes. Dotted line indicates HRU processes.

1.3 Spatial data and Hydrologic Response Units (HRUs)

1.3.1 Input climate data

The spatial resolution of AWRA-L is driven by the resolution of input climate data, namely 0.05° (approximately 5 km).

AWRA-L uses the daily gridded Australian Water Availability Project (AWAP) climate data set that consists of air temperature (daily minimum and maximum) and daily precipitation from 1st January 1911 to yesterday (Jones et al., 2009).

The rainfall and temperature data are interpolated from station records and provided on a 0.05° grid across Australia. Additionally, daily solar exposure (downward shortwave radiation) is produced from geostationary satellites (Grant *et al.*, 2008) and aggregated to the same 0.05° AWAP grid. The solar radiation record is from 1990 to yesterday, with the Himawari-8 satellite used since 23rd March 2016. Prior to that date the GMS-4, GMS-5, GOES-9 and MTSAT-1R satellites were used. Daily climatological averages (taken for each month) are used for solar radiation prior to 1990.

Site based daily wind run observations collated by the Bureau of Meteorology and interpolated nationally using the method developed by McVicar *et al.* (2008) were used for daily average wind speed in AWRA-L v6 from 1975 onwards (when sufficient site observations were being collated by the Bureau). A daily varying climatology value, based on the period 1975-2017, was used prior. This differs from AWRA-L v5 and previous versions where this daily data was averaged temporally (Figure 3) to generate a single daily average value that applied at all timesteps.
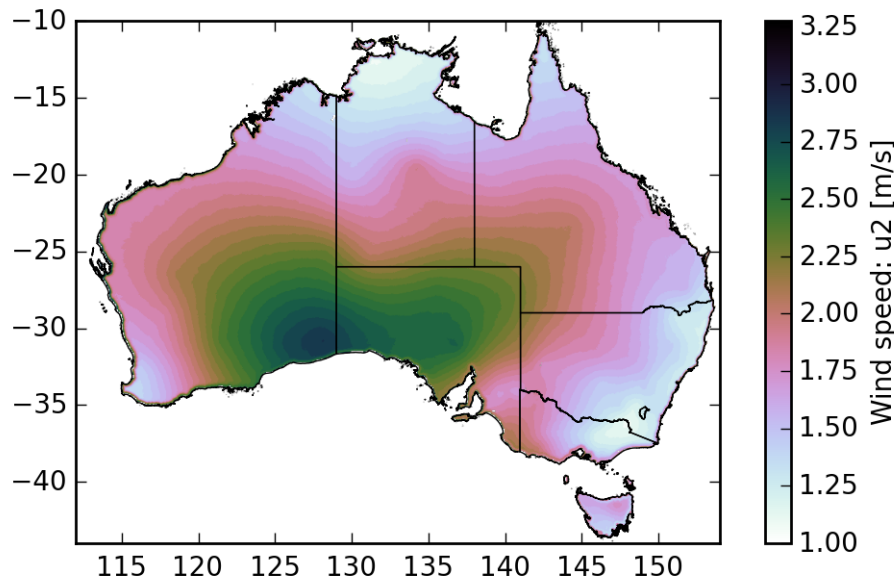
Figure 3. AWRA-L v5 Wind speed climatology (u_2)

The following notation is used for the climate forcing in this report:

P_g Daily gross precipitation to 9am local time [mm]

K_d Daily downwelling shortwave (solar) radiation [MJ m^{-2} d^{-1}]

u_2 Wind speed at a height of 2 m [m/s]

T_{min} Daily minimum air temperature to 9am local time [°C]

T_{max} Daily maximum air temperature from 9am local time [°C]

It is noted that the daily minimum and maximum air temperature actually cover two adjacent days (a period of 48 hours) and it is possible to have $T_{min} > T_{max}$. A weighted average of these two values is taken to get an average temperature value for calculation of Potential Evaporation, with the T_{min} being set to T_{max} in cases where $T_{min} > T_{max}$ – see section 3.1.

1.3.2   Static spatial datasets

Various static spatial datasets are used to parameterise AWRA-L spatially. These spatial grids (discussed subsequently within the document) are as follows:

f_{tree} The HRU proportion of deep rooted vegetation in each cell (Figure 4). The remaining HRU proportion (1- f_{tree}) is assumed shallow rooted vegetation within each grid cell (see section 1.3.3)

P_{refmap} Reference precipitation [mm/d] controlling infiltration-excess runoff further derived from slope β and $K_{0satPEDO}$ using an empirical relationship (see section 2.1.1). Figure 6 shows the final value used in AWRA-L v6 after scaling of the mapped value according to model parameter optimisation.

$K_{xsatPEDO}$ Saturated hydraulic conductivity [mm/d] for the top (x=0), shallow (x=s) and deep (x=d) layers defining the drainage rate when saturated (see section 2.1.2). These values were derived using pedotransfer functions based on clay content. Figure 7 shows the final value used in v6 after scaling of the mapped values according to model parameter optimisation.

S_{xAWC} Available water storage fraction for top (x=0), shallow (x=s) and deep (x=d) layers (see section 2.1.2). These values were derived from available mapping. Figure 7 shows the final value used in v6 after scaling of the mapped values according to model parameter optimisation.

β Slope of the land surface [percent] derived according to Digital Elevation Model (DEM) analysis (Figure 8). Slope affects infiltration excess runoff (through Reference precipitation P_{ref} ; see section 2.1.1) and the proportion of drainage that occurs laterally as interflow (section 2.1.2).

K_{gmap} The groundwater drainage coefficient controls the baseflow rate – see section 2.1.3. Figure 9 shows the final value used in v6 after scaling of the mapped values according to model parameter optimisation.

n_{map} Effective porosity affects lateral groundwater flow (baseflow; through K_{gmap}), along with the fraction saturated groundwater (which effects the amount of saturated overland flow) and fraction of groundwater available transpiration (Figure 10)

Hypsometric curves   The hypsometric curve is the cumulative distribution of elevation within an AWRA-L grid cell, based on a finer scale DEM. This is used for conversion from groundwater storage to head relative to the lowest point in the cell. The head level determines the fraction saturated

groundwater (which effects the amount of saturated overland flow) and fraction of groundwater available transpiration – see section 2.1.3.

$\overline{E^*}$ Long term mean daily evapotranspiration is related by and empirical equation to the routing delay for streamflow (Figure 12)

h_{veg} Vegetation height of deep rooted vegetation (i.e. to the top of the canopy for tall vegetation and derived from lidar estimates) alters the aerodynamic conductance (Figure 13)

LAI_{max} Maximum leaf area index (Figure 14) defines the maximum achievable canopy cover in a particular cell.

The figures referenced above show the resulting parameters used in AWRA-L, often according to a transformation of scaling undertaken as a result of the calibration process.

1.3.3 HRU proportions (f_{tree})

Each spatial unit (grid cell) in AWRA-L is divided into a number of hydrological response units (HRUs) representing different landscape components. Hydrological processes (with the exception of groundwater storage) are modelled separately for each HRU before the resulting fluxes are combined to give cell outputs, by a weighted sum according to the proportion of each HRU. The current version of AWRA-L includes two HRUs which notionally represent (i) tall, deep-rooted vegetation (i.e., forest), and (ii) short, shallow-rooted vegetation (i.e., non-forest). Hydrologically, these two HRUs differ in their aerodynamic control of evaporation, in their interception capacities and in their degree of access to different soil layers.

The fraction of tree cover within each grid cell (denoted f_{tree}) is used to apportion the grid cell area to each of the two HRUs: shallow rooted versus deep rooted vegetation. It is based on the Advanced Very High Resolution radiometer (AVHRR) satellite derived fractions of persistent and recurrent photosynthetically active absorbed radiation (fPAR) (Donohue, Roderick and McVicar, 2008) where persistent vegetation is interpreted to be tree cover (deep rooted) and recurrent vegetation is interpreted to be grass cover (shallow rooted) (Figure 4). The tree fraction is assumed to remain static throughout the simulation.
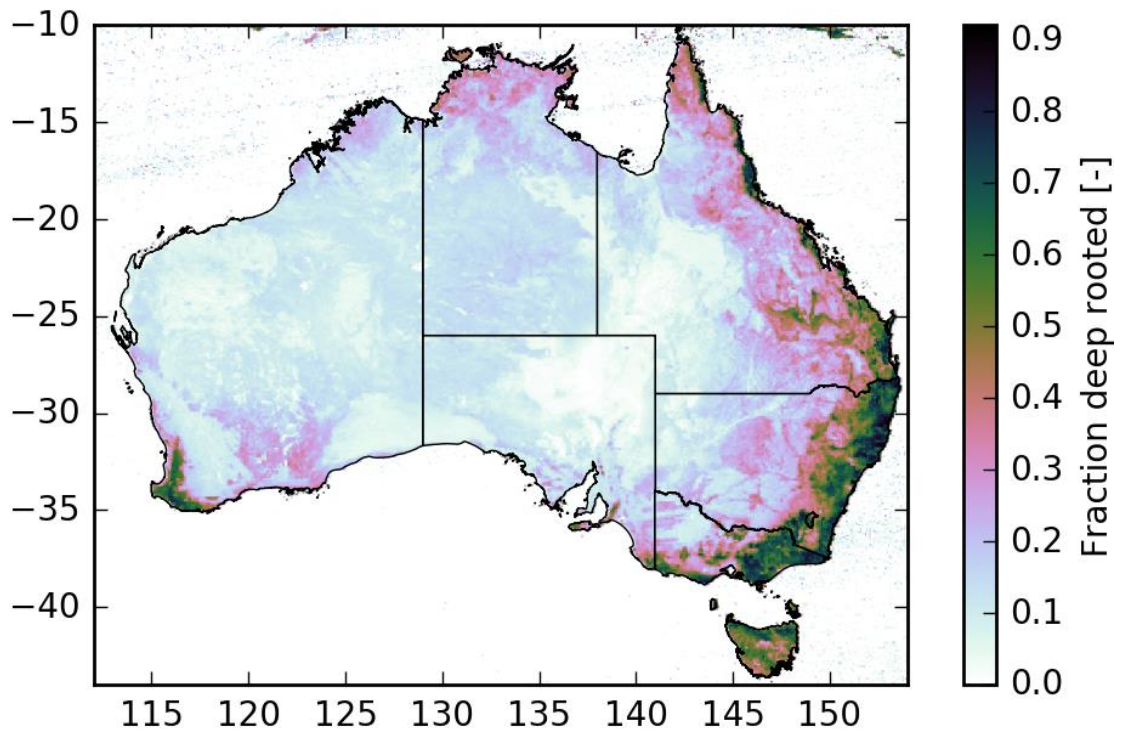
Figure 4. Fraction deep rooted vegetation within each grid cell (f_{tree})

1.4 Structure of this report

This report is structured according to the three functional components of the model shown in Figure 2:

- Chapter 2: Water balance
- Chapter 3: Vapour fluxes and the energy balance
- Chapter 4: Vegetation phenology
- Chapter 5: Parameterisation

2 Water balance

Figure 5 shows a conceptual diagram of the water balance processes modelled in AWRA-L. These processes are described in this section.
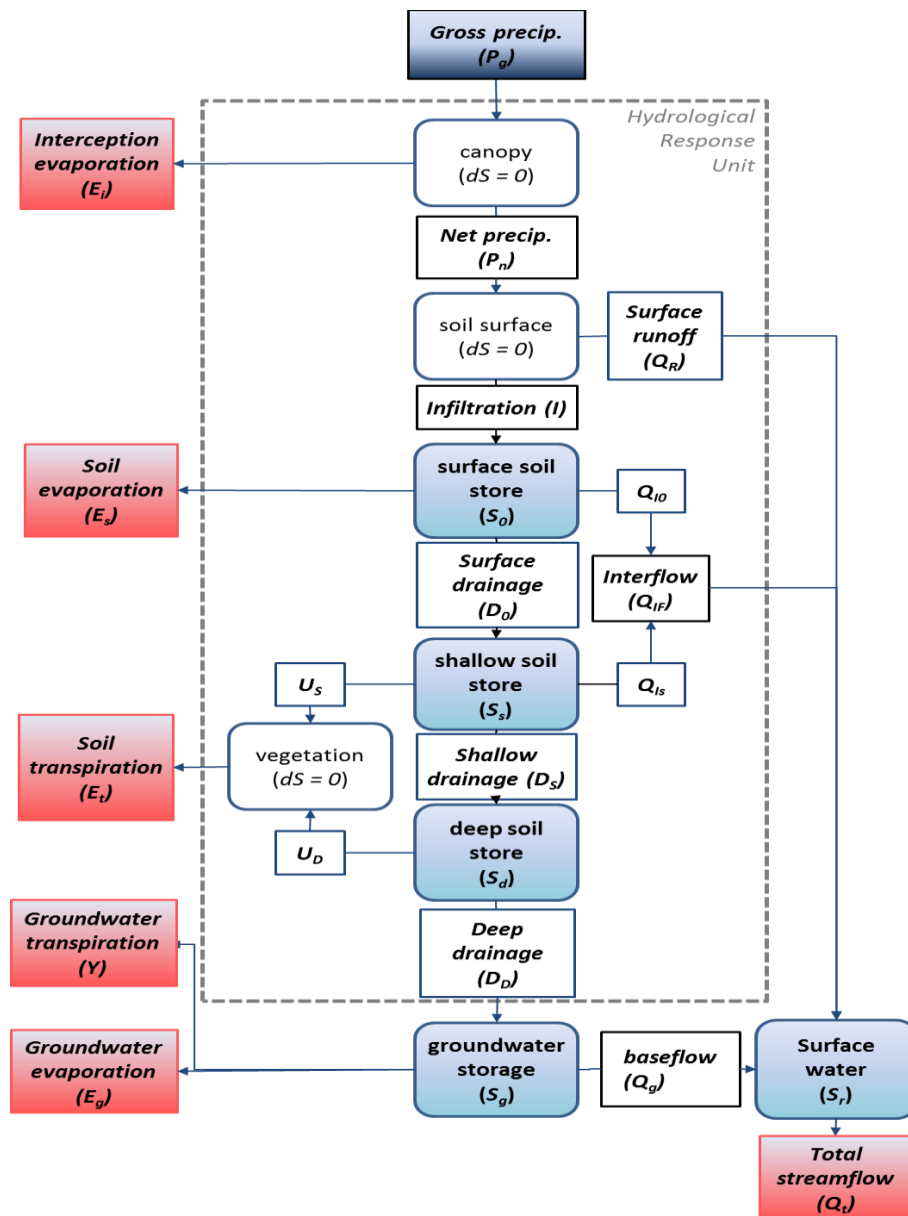
Figure 5. AWRA-L hydrological processes. Blue rounded boxes indicate water storages, white if no storage, white boxes are water balance fluxes, and red boxes are the output fluxes.

2.1 Water balance equations

All water storage and daily flux terms have millimetres [mm] for units. Throughout the document (*t*) is used to denote the value corresponding to day t. All calculations below are undertaken for the shallow and deep rooted HRUs separately, with the exception of the groundwater balance (considered as a single store) and total stream discharge (which are from a weighted sum of the flows over the two HRUs).

Gross rainfall (P_g) [mm] from the interpolated gridded daily input data after subtracting evaporation due to canopy interception (E_i), assuming no canopy storage, gives the net rainfall (P_n):

$$P_n(t) = \begin{cases} P_g(t) - E_i(t), & P_g > E_i \\ 0, & P_g \le E_i \end{cases} \tag{1}$$

Soil surface partitioning of net rainfall into surface runoff (Q_R) and infiltration (I) gives:

$$I(t) = P_n(t) - Q_R(t) \tag{2}$$

Top soil water balance, comprising top soil water storage (S_0), infiltration, soil evaporation (E_s), interflow draining laterally from the top soil layer (Q_{I0}) and top soil drainage (D_0):

$$S_0(t) = S_0(t-1) + I(t) - D_0(t) - Q_{I0}(t) - E_s(t) \tag{3}$$

Shallow soil water balance, comprising shallow soil water storage (S_s), shallow root water uptake (U_s), top soil drainage (D_0) from the layer above, interflow draining laterally from the shallow soil layer (Q_{Is}) and shallow soil water drainage (D_s):

$$S_s(t) = S_s(t-1) + D_0(t) - D_s(t) - Q_{Is}(t) - U_s(t) \tag{4}$$

Deep soil water balance, comprising deep soil water storage (S_d), D_s, deep root water uptake (U_d), and deep drainage (D_d):

$$S_d(t) = S_d(t-1) + D_s(t) - D_d(t) - U_d(t) \tag{5}$$

Groundwater balance, comprising ground water storage (S_g), D_d, root water uptake from groundwater store (Y), groundwater evaporation (E_g) and groundwater discharge (Q_g):

$$S_g(t) = S_g(t-1) + \boldsymbol{D_d}(t) - \boldsymbol{Q_g}(t) - \boldsymbol{E_g}(t) - \boldsymbol{Y}(t) \tag{6}$$

with each flux component a weighted sum according to the fraction HRU – denoted in bold here.

River water balance, comprising surface water storage (S_r), surface runoff (Q_R), interflow ($Q_I = Q_{I0} + Q_{Is}$), baseflow (Q_g), and total stream discharge (Q_t):

$$S_r(t) = S_r(t-1) + \boldsymbol{Q_R}(t) + Q_g(t) + \boldsymbol{Q_I}(t) - Q_t(t) \tag{7}$$

2.1.1 Surface runoff ($Q_R = Q_h + Q_s$)

Gross rainfall following canopy interception evaporation (see section 3.3 for all vapour fluxes) gives net precipitation (P_n), which is further partitioned into surface runoff (Q_R) and infiltration (I) in eqn (2).

Surface runoff ($Q_R = Q_h + Q_s$), is calculated as the sum of an infiltration-excess runoff component, Q_h, and a saturation-excess runoff component, Q_s.

All precipitation falling on the saturated fraction [-] of the landscape (f_{sat}) is assumed to run off, as saturation excess as per:

$$Q_s(t) = f_{sat}(t)P_n(t) \tag{8}$$

where calculation of the fraction of saturated area (f_{sat}) is dependant of the groundwater storage (S_g) relative to the topography as defined by the hypsometric curves – see section 2.1.3.

Infiltration-excess runoff is assumed to be generated from the unsaturated fraction ($1 - f_{sat}$) of the landscape at a rate that is modulated by the reference precipitation parameter P_{ref}:

$$Q_h(t) = \left(1 - f_{sat}(t)\right)\ \left(P_n(t) - P_{ref}\tanh\frac{P_n(t)}{P_{ref}}\right) \tag{9}$$

P_{ref} (Figure 6) represents the daily net precipitation amount at which approximately 76% of the net precipitation becomes infiltration excess runoff (Viney et $al.$, 2015).

The original form of these equation was chosen by (Van Dijk, 2010b; Van Dijk, 2010c) based on analysis of several different alternatives – that used a single value of P_{ref} spatially. Subsequent development introduced P_{ref} as an empirical function of the saturated hydraulic conductivity of surface soil ($K_{0satPEDO}$) and slope [percent] (β):

$$P_{ref} = P_{refscale} * P_{refmap} \tag{10}$$

where

$$P_{refmap} = 20\ \left(2 + \log\left(\frac{K_{0satPEDO}}{\beta}\right)\right)$$

Following calculation of the surface runoff the infiltration component (I) is given by eqn (2).
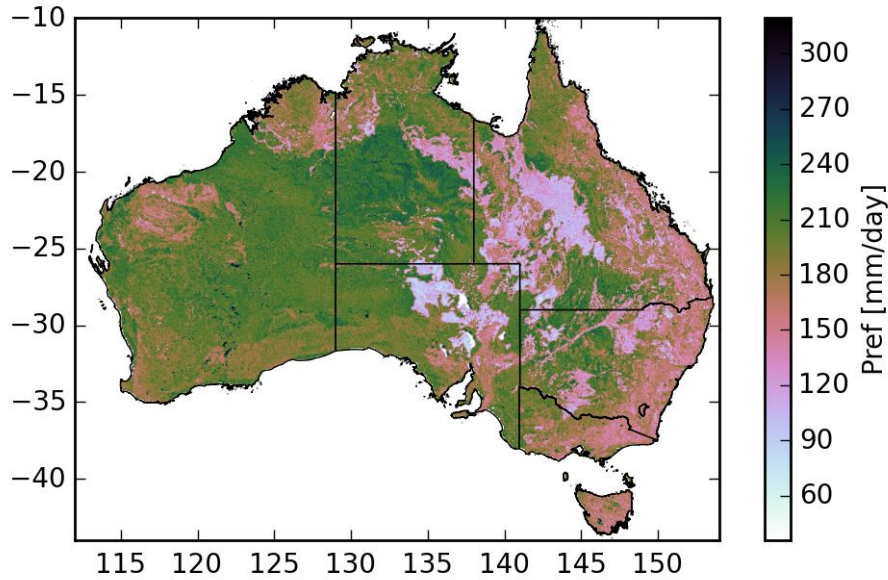
Figure 6. Continental distribution of reference precipitation $\left(P_{ref}\right)$.

2.1.2 Soil storage (S_0, S_s, S_d), drainage (D_0, D_s, D_d) and interflow $(Q_{IF} = Q_{I0} + Q_{Is})$

Total soil drainage (including vertical drainage and interflow) is assumed to occur according to the following equations for each soil layer.

For the top soil layer drainage (D_0) and lateral interflow (Q_{I0}):

$$D_0(t) + Q_{I0}(t) = K_{0sat} \left(\frac{S_0(t)}{S_{0max}}\right)^2 \tag{11}$$

Shallow soil layer drainage (D_s) and lateral interflow (Q_{Is}):

$$D_s(t) + Q_{Is}(t) = K_{ssat} \left(\frac{S_s(t)}{S_{smax}}\right)^2 \tag{12}$$

Deep soil layer drainage (D_d) assuming no lateral interflow from that layer:

$$D_d(t) = K_{dsat} \left(\frac{S_d(t)}{S_{dmax}}\right)^2 \tag{13}$$

Where K_{xsat} and S_{xmax} represents the saturated hydraulic conductivity [mm/day] and maximum storage [mm] of the relevant soil layer *x*.

The spatial maps of these parameters are shown in Figure 7. These drainage parameters are derived from the following equations:

$$S_{0max} = d_0 S_{0AWC} S_{0maxscale} \tag{14}$$

$$S_{smax} = d_s S_{sAWC} S_{smaxscale} \tag{15}$$

$$S_{dmax} = d_d S_{dAWC} S_{dmaxscale} \tag{16}$$

$$K_{0sat} = K_{0satscale} K_{0satPEDO} \tag{17}$$

$$K_{ssat} = K_{ssatscale} K_{ssatPEDO} \tag{18}$$

$$K_{dsat} = K_{dsatscale} K_{dsatPEDO} \tag{19}$$

Where d_0, d_s and d_d is the depth of the top, shallow and deep soil layers (100mm, 900mm, 5000mm), S_{0AWC}, S_{sAWC} and S_{dAWC} is the (proportional) available water holding capacity of the top and shallow layers as the plant available water capacity of a layer divided by its thickness). $K_{xsatPEDO}$ are the saturated hydraulic conductivities of the relevant soil layers.

Available water capacities and saturated hydraulic conductivities are derived from pedotransfer functions applied to the continental scale mapping of clay content from the Soil and Landscape Grids of Australia (http://www.clw.csiro.au/aclep/soilandlandscapegrid). The pedotransfer function of Dane and Puckett (1994) was used for estimation of saturated conductivity $(K_{xsatPEDO})$ for each level:

$$K_{satPEDO} = 303.84 \exp(-0.144 P_{<2})$$

Where $P_{<2}$ is the clay fraction (ie. < 2 um mass fraction of the < 2 mm soil material determined using the pipette method). This pedotransfer function was recommended by Minasny and McBratney (2000) according to evaluation and comparison to other methods using Australian soil data.

Available water capacity was derived based on pedotransfer functions for soil water retention at field capacity (θ_{-33}: with -33kPa interpreted as the soil's capacity in the field to retain water) and wilting point (θ_{-1500}: with -1500kPa interpreted as the amount of water in the soil which will cause a plant to wilt):

$$S_{AWC} = \theta_{-33} - \theta_{-1500}$$

The following pedotransfer functions produced by Minasny *et al.* (1999) were used to estimate each of these components:

$$\theta_{-33} = 0.3543(1 - exp(-0.0385 P_{<2})) + 0.083$$

$$\theta_{-1500} = 0.4016(1 - exp(-0.0230 P_{<2})) + 0.0027$$

Further details of the approach for derivation of these spatial layers is described in Vaze *et al.* (2018); although there are marginal differences to the layers described in that report as the grids were derived directly by the Bureau of Meteorology.

The relative soil moisture w_x content of the soil layers (top, shallow and deep) are required subsequently in various process calculations and is given by:

$$w_\text{x}(t) = \frac{S_\text{x}(t)}{S_{\text{x }max}} \tag{20}$$

Where S_x is the soil storage and $S_{\text{x }max}$ is the maximum storage for layer x.
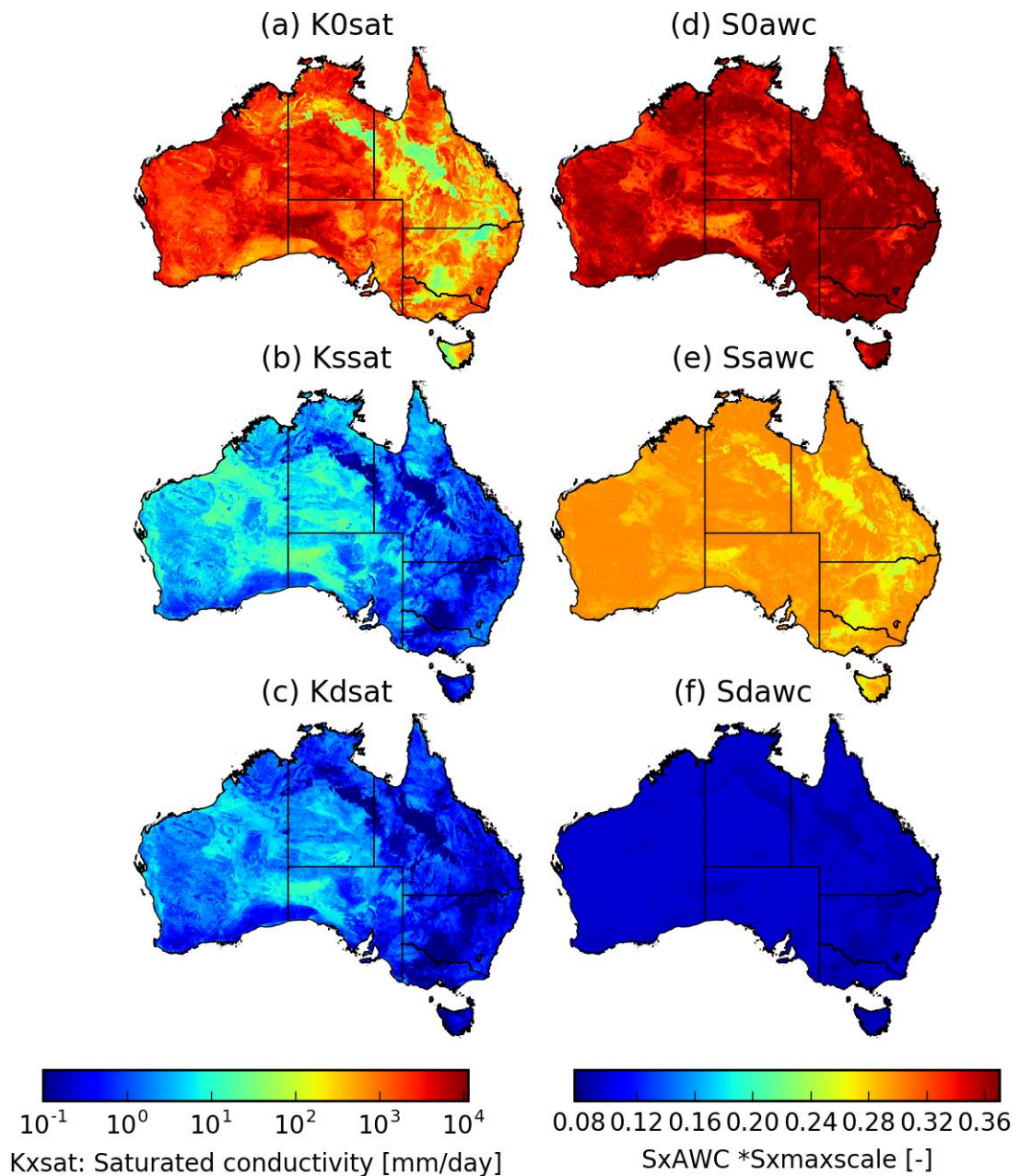
Figure 7. Saturated conductivity (K_{xsat}) and proportion available water capacity ($S_{sAWC}S_{smaxscale}$) for the top (0), shallow (s) and deep (d) soil layers.

Total drainage for each layer (defined by the right hand side of Eqns 11-12) are partitioned into the drainage and interflow components (left hand side of Eqns 11-12) according to the following equations.

The proportion of overall top layer drainage that is lateral/interflow drainage (ρ_0) is given by:

$$\rho_0(t) = \tanh(k_\beta \beta \frac{S_0(t)}{S_{0max}}) \tanh\left(k_\zeta \left(\frac{K_{0sat}}{K_{ssat}} - 1\right) \frac{S_0(t)}{S_{0max}}\right) \tag{21}$$

The proportion of drainage that is lateral/interflow drainage for the shallow layer (ρ_s) is given by:

$$\rho_s(t) = \tanh(k_\beta \beta \frac{S_s(t)}{S_{smax}}) \tanh\left(k_\zeta \left(\frac{K_{ssat}}{K_{dsat}} - 1\right) \frac{S_s(t)}{S_{smax}}\right) \tag{22}$$

Where β is the slope [radians] (noting radians are used here rather than percent elsewhere), k_β is a dimensionless scaling factor and k_ζ is a scaling factor for ratio of saturated hydraulic conductivity. The forms of the partitioning factor equations were chosen so that the proportion of drainage to interflow increases with increasing slope, soil moisture and the conductivity difference at the interface of the soil layers.

The slope (see Figure 8) values were derived by calculating average values from a 3 second DEM analysis (Viney *et al.*, 2015).
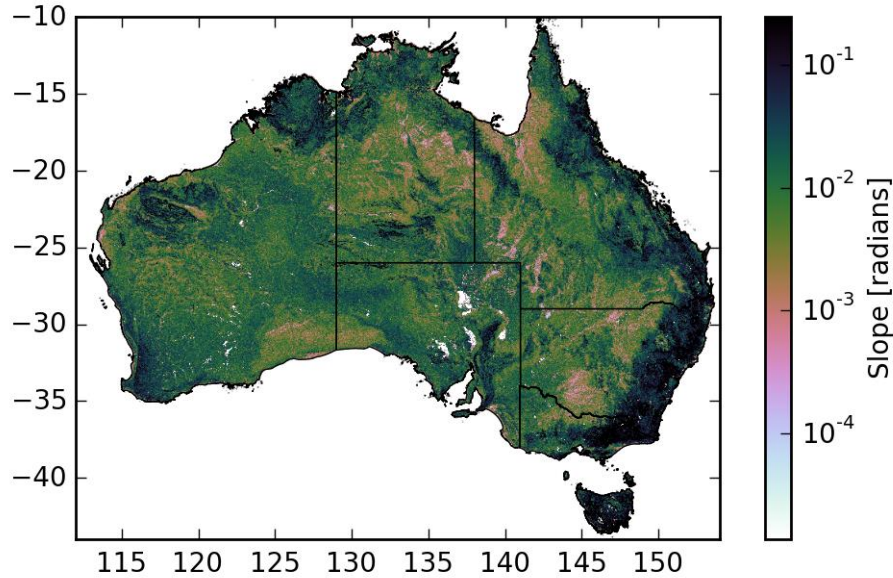
Figure 8. Average slope (β) within a grid from a 3 second DEM

Total interflow (Q_{IF}) from the top and shallow soil layers is given by the sum:

$$Q_{IF} = Q_{I0} + Q_{Is} \tag{23}$$

2.1.3 Groundwater storage (S_g) and fluxes (Q_g, E_g, Y)

Groundwater balance (defined in Eqn (6)), comprises ground water storage (S_g), D_d, root water uptake from groundwater store (Y), groundwater evaporation (E_g) and groundwater discharge (Q_g).

Groundwater discharge to stream (baseflow) is conceptualised as a linear reservoir with the discharge being proportional to S_g according to:

$$Q_g(t) = \max(S_g(t-1) + \boldsymbol{D_d}(t), 0) * (1 - e^{-K_g}) \tag{24}$$

Where K_g is the Groundwater drainage coefficient:

$$K_g = K_{gscale}\, K_{gmap} \tag{25}$$

K_{gmap} is the groundwater drainage coefficient obtained from continental mapping and K_{gscale} is an optimised scaling factor.

Baseflow only occurs when the storage level is above the drainage base H_b– the lowest topographic point in the cell (see section on hypsometric curves below).

The one-parameter formulation chosen here (from analysis presented in Van Dijk, 2010a) is known as a linear reservoir equation and is commonly used in lumped catchment rainfall-runoff models (Van Dijk, 2010c).
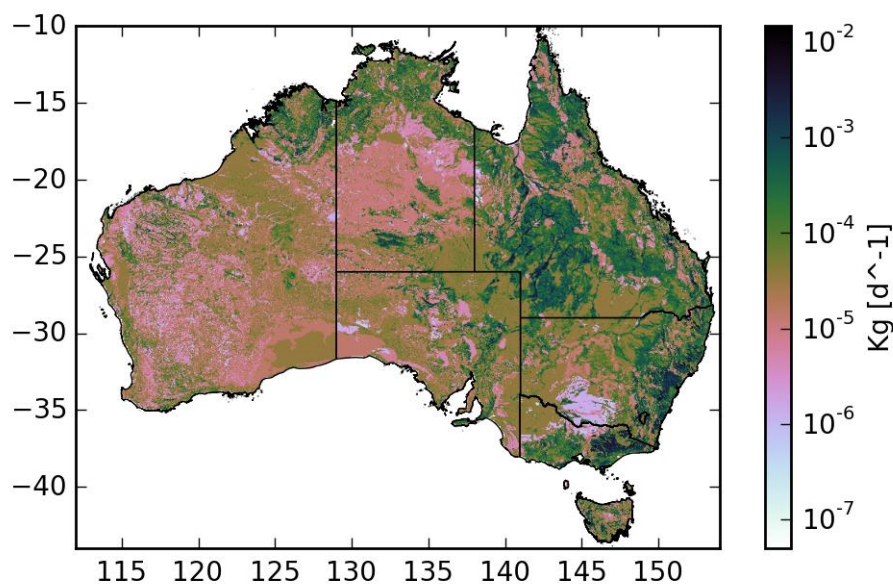
Figure 9. Groundwater drainage coefficient (K_g)

K_{gmap} is derived from the depth to the unconfined aquifer (d_u), the elevation change along the flow path (h_u), and from continental mapping of surface water drainage density (λ_d) (not shown) and the effective porosity (n_{map}):

$$K_{gmap} = \frac{k_u (2\lambda_d)^2 \max\{d_u, h_u\}}{n_{map}} \tag{26}$$

Groundwater evaporation and transpiration are dependent on the fraction of the grid cell that is saturated at the surface (f_{sat}) and the fraction of the grid cell that is accessible for transpiration (f_{Eg}). Both of these values are functions of the groundwater head (h) relative to the cumulative distribution of topography (termed hypsometric curves) within the cell (Peeters *et al.*, 2013). In AWRA v6, distribution is based on a finer scale SRTM based DEM (1 second; see DEM_S in https://data.gov.au/dataset/srtm-derived-1-second-digital-elevation-models-version-1-0).

Groundwater storage (S_g) in mm is converted to head (in metres) according to:

$$S_g(t) = 1000nh(t) \tag{27}$$

Effective porosity (n) [-] is given by:

$$n = n_{scale}\, n_{map} \tag{28}$$

where n_{map} is effective porosity obtained from continental mapping and n_{scale} is the scaling factor for effective porosity.
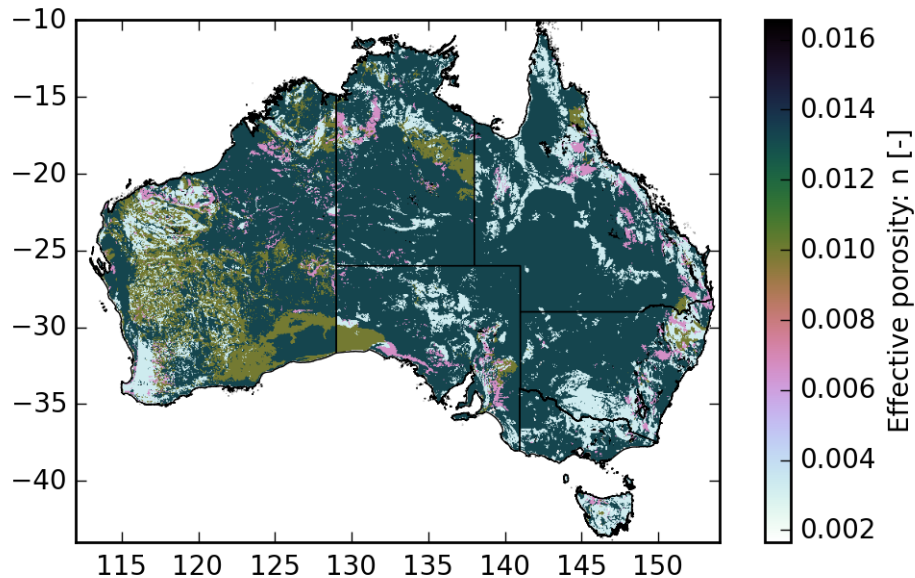
Figure 10. Effective porosity (n)

The fraction of the grid cell where the water table is above the ground surface is considered to be the saturated area. Thus, f_{sat} [-] is taken as the fraction on the cumulative curve at which elevation is equal to $1000nH_b + S_g$. H_b is the drainage base [m] – the lowest topographic point within the grid cell.

Similarly, the fraction of a grid cell that is accessible for the vegetation to transpire groundwater (f_{Eg}) is calculated as the fraction of the grid cell where the water table is above a plane of the rooting depth of the vegetation below the surface elevation. That is, where the elevation is equal to $1000n(H_b + D_R) + S_g$ where D_R is the rooting depth [m]: currently set to the depth of the base deep rooted vegetation within the deep soil store (6m).
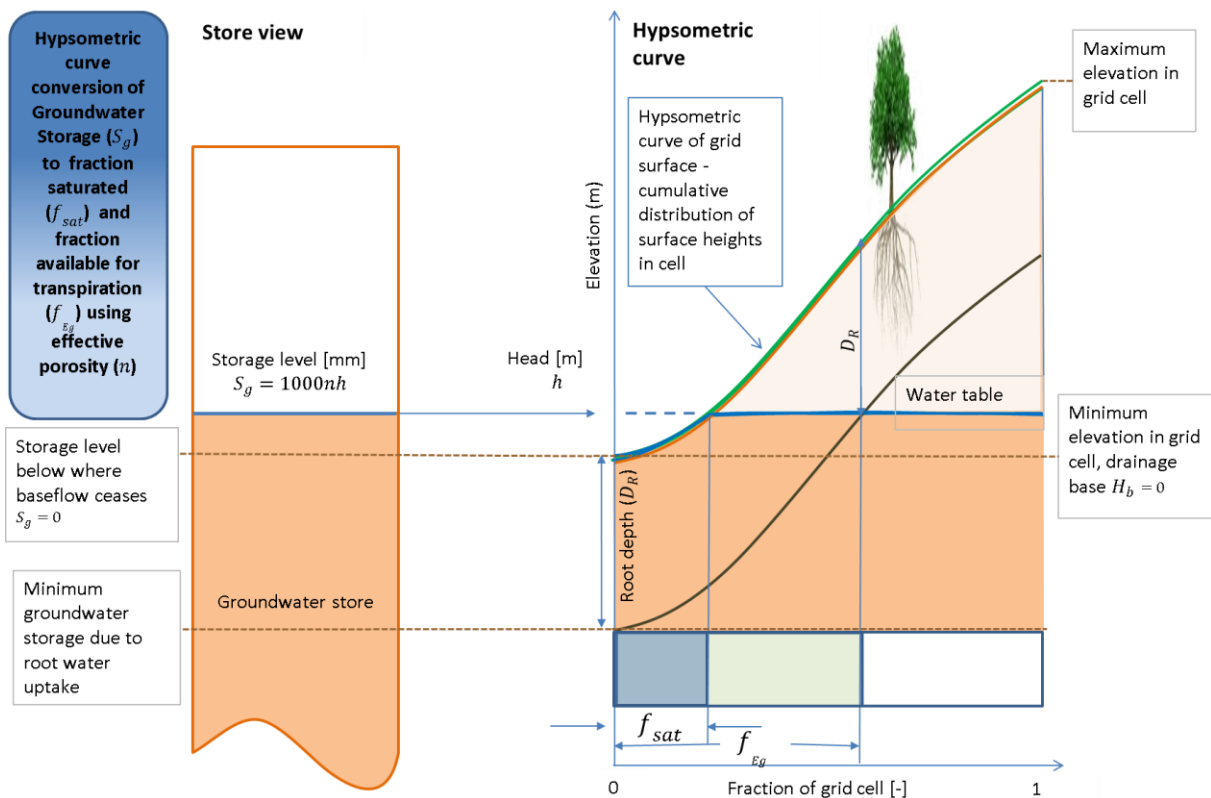
Figure 11. Hypsometric curve conversion of groundwater storage to fraction of cell saturated and fraction of cell available for transpiration

20

2.1.4 Total Streamflow and surface water storage

In AWRA-L, streamflow (Q_t) is sourced from surface runoff, baseflow and interflow according to Eqn (7). Discharge of water from these sources is routed via a notional surface water store, S_r (mm). The purpose of this store is primarily to reproduce the partially delayed drainage of storm flow that is normally observed in all but the smallest and fastest responding catchments.

The discharge from this surface water store is controlled by a routing delay factor (K_r) according to:

$$Q_t(t) = (1 - e^{K_r}) \left(S_r(t - 1) + Q_h(t) + Q_s(t) + Q_g(t) + Q_I(t) \right) \tag{29}$$

Where the routing delay is calculated via a linear relationship with long term mean daily evapotranspiration ($\overline{E^*}$)

$$K_r = K_{rint} + K_{rscale}\overline{E^*} \tag{30}$$

where K_{rint} is an Intercept coefficient and K_{rscale} is a scale coefficient for calculating K_r. This relationship was chosen based on empirical analysis over 260 Australian catchments presented in Van Dijk (2010c, 2010b). It is noted that the two parameters in Eqn 30 are optimised.
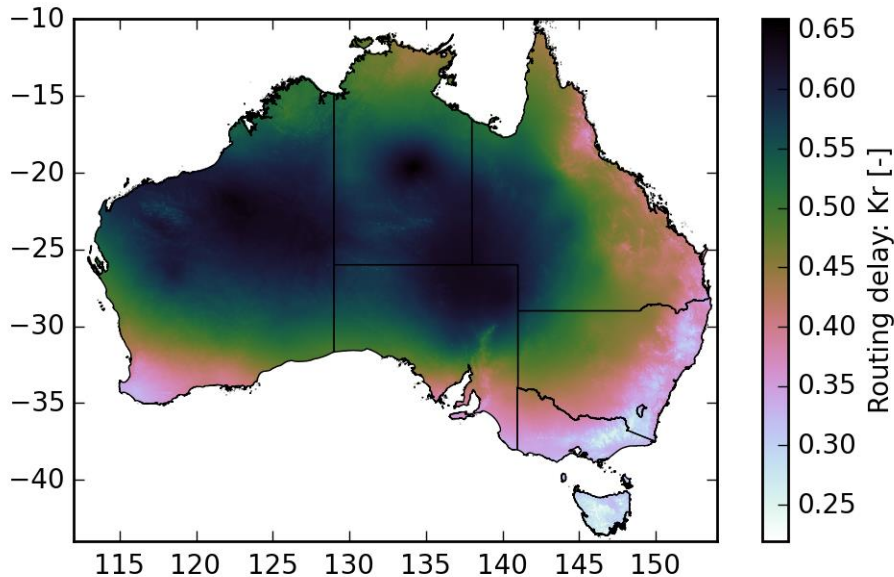
Figure 12. Streamflow routing coefficient (K_r)

3 Vapour fluxes and the energy balance

3.1 Potential evaporation (E_0)

An estimate of potential evaporation is a key element of the landscape modelling in AWRA-L. Potential evaporation is required to scale, and to provide an upper limit on, evaporation and transpiration processes from the soil and vegetation (see section 3.3).

Potential evaporation E_0 [mm/day] is calculated according to the Penman (1948) equation (Viney *et al.*, 2015) as a combination of net radiation (the energy required to sustain evaporation) and vapour pressure deficit (multiplied by a wind function)

$$E_0(t) = \max\left\{0, \frac{\Delta(t)R_n(t) + 6.43\gamma[p_{es}(t) - p_e(t)][1 + 0.546u_2(t)]}{\lambda(t)[\Delta(t) + \gamma]}\right\} \tag{31}$$

where Δ [Pa/K] is the slope of the saturation vapour pressure curve, R_n [MJ m^{-2} d^{-1}] net radiation, γ [Pa/K] the psychometric constant, λ [MJ/kg] the latent heat of vaporisation, u_2 is wind speed at a height of 2 m [m/s], p_{es} [Pa] is saturation vapour pressure and p_e is actual vapour pressure [Pa]. Since Equation (31) is intended to apply at a daily time step, the soil heat flux is assumed to be negligible in comparison with the net radiation flux, and is therefore ignored.

The latent heat of vaporisation λ is given by Shuttleworth (1992); Allen *et al.*(1998) as:

$$\lambda(t) = 2.501 - 0.002361T_a(t) \tag{32}$$

where T_a [°C] is daily mean temperature, taken to be the weighted mean of the daily maximum (T_{max}) and minimum (T_{min}) temperature (Raupach *et al.*, 2008):

$$T_a(t) = \begin{cases} 0.75T_{max}(t) + 0.25T_{min}(t) & \text{if } T_{min}(t) \leq T_{max}(t) \\ T_{max}(t) & \text{if } T_{min}(t) > T_{max}(t) \end{cases} \tag{33}$$

As Van Dijk (2010c) notes, several of the temperature-dependent functions used are strongly non-linear and therefore the above approximation will possibly introduce error, although its magnitude is unknown.

The slope of the saturation vapour pressure curve is:

$$\Delta(t) = 4217.457 \frac{p_{es}(t)}{\left(240.97 + T_a(t)\right)^2} \tag{34}$$

Saturation vapour pressure (p_{es}) is given according to the following approximation (Shuttleworth, 1992):

$$p_{es}(t) = 610.8 \exp\left(\frac{17.27T_a(t)}{237.3 + T_a(t)}\right) \tag{35}$$

Actual vapour pressure is calculated (using the same equation) on the assumption that the air is saturated at night when the air temperature is at its minimum and that this actual vapour pressure remains constant throughout the day:

$$p_e(t) = 610.8 \exp\left(\frac{17.27T_{min}(t)}{237.3 + T_{min}(t)}\right) \tag{36}$$

3.2 The energy balance

Potential evaporation depends on the available energy at the surface, which is given by the net radiation term (R_n) [MJ/m²/day]. This term, in turn, requires estimation of its constituent upward and downward fluxes of shortwave and longwave radiation:

$$R_n(t) = K_d(t) - K_u(t) + L_d(t) - L_u(t) \tag{37}$$

where K_d is downward (incoming) solar radiation, K_u the reflected outgoing shortwave radiation, L_d the cloud reflected downward (incoming) longwave radiation and L_u the outgoing terrestrial radiation. As E_0 is intended to apply at a daily time step, the soil heat flux is assumed to be negligible in comparison with the net radiation flux, and is therefore ignored.

3.2.1 Upward and Downward shortwave radiation

Downward shortwave radiation K_d [MJ/m²/day] is given according to the gridded input solar radiation data (section 1.3.1). The upward shortwave radiation K_u [MJ/m²/day] is calculated from K_d and the land surface albedo α [-]:

$$K_u(t) = \alpha(t)K_d(t) \tag{38}$$

where

$$\alpha(t) = f_v(t)\alpha_v + f_s(t)\alpha_s(t) \tag{39}$$

with f_v [-] the fractional canopy cover, α_v [-] the vegetation albedo, f_s [-] is the fraction of soil cover, and α_s [-] the soil albedo.

Fractional canopy cover f_v estimation is discussed in Section 4 (Vegetation Phenology). The fraction of soil cover is the portion that is not living vegetation and includes soil, rock, dead biomass and other land cover:

$$f_s(t) = 1 - f_v(t) \tag{40}$$

The vegetation albedo α_v [-] is calculated from the vegetation photosynthetic capacity index (per unit canopy cover) V_c [-] as:

$$\alpha_v = 0.452V_c \tag{41}$$

The relationship was derived using MODIS broadband white sky albedo and the photosynthetic capacity index V_c was calculated from MODIS Enhanced Vegetation Index, with MODIS fPAR used to estimate the fractional canopy cover f_v. In the model V_c is a parameter fixed to 0.65 and 0.35 for shallow and deep rooted vegetation (respectively) – see Van Dijk (2010c).

The soil albedo α_s [-] is calculated from the wet soil albedo α_{wet} [-] and the dry soil albedo α_{dry} [-]

$$\alpha_s(t) = \alpha_{wet} + (\alpha_{dry} - \alpha_{wet})e^{-\left(\frac{w_0(t)}{w_{0\,ref}}\right)} \tag{42}$$

where the relationship between albedo and surface soil moisture was derived using MODIS broadband white sky albedo and ASAR surface soil moisture. In the model the wet soil albedo α_{wet} [-], dry soil albedo α_{dry} [-], and the reference value of w_0 (determining the rate of albedo decrease with wetness) $w_{0\,ref}$ [-] are parameters fixed to 0.16, 0.26 and 0.3 (respectively), with the same parameter used for both shallow and deep rooted vegetation (Van Dijk, 2010c).

3.2.2 Upward longwave radiation

Upward longwave radiation L_u [W/m²] is calculated according to black body theory with the terrestrial surface radiation given as $\varepsilon\sigma T^4$. Assuming a surface emissivity ε of 1 (Van Dijk, 2010c) and using the air temperature T_a [°C] as an estimate of the surface temperature [°K] gives

$$L_u(t) = \sigma(T_a(t) + 273.15)^4$$

with σ [W/m²/K⁴] the Stefan-Boltzmann constant represented as 5.67x10⁻⁸ in the model (Dong *et al.*, 1992; Donohue, McVicar and Roderick, 2009).

3.2.3 Downward longwave radiation

The downward longwave radiation L_d [W/m²] is calculated from:

$$L_d(t) = \sigma(T_a(t) + 273.15)^4 \left\{ 1 - \left[1 - 0.65 \left(\frac{e_a(t)}{T_a(t) + 273.15} \right)^{0.14} \right] \left(1.35 \frac{K_d(t)}{K_{d0}(DOY)} - 0.35 \right) \right\}$$

Where K_{d0} is the expected downwelling shortwave radiation on a cloudless day (MJ m⁻² d⁻¹) as a function of the numeric day of the year (DOY), latitude (ϕ) [radians], solar declination δ [radians] and ω the sunset hour angle [radians]:

$$K_{d0}(DOY) = \frac{94.5 \left(1 + 0.033 \cos\left(\frac{2\pi DOY}{365} \right) \right)}{\pi} (\omega \sin\delta \sin\phi + \cos\delta \cos\phi \sin\omega)$$

$$\delta = 0.006918 - 0.39912 \cos(Q_0) + 0.070257 \sin(Q_0)$$
$$- 0.006758 \cos(2Q_0) + 0.000907 \sin(2Q_0)$$
$$- 0.002697 \cos(3Q_0) + 0.00148 \sin(3Q_0)$$

$$Q_0 = \frac{2\pi(DOY - 1)}{365}$$

This is similar to the equation for L_d in Donohue et al. (2009), but with different parameterisations for the atmospheric emissivity and transmissivity for a clear sky. It is noted that this is different from the initial derivation provided by Van Dijk (2010c), as

downwelling longwave radiation is now augmented by radiation from the cloud base (see Viney et al, 2015). The derivation is detailed in Appendix B.

3.3 Actual evapotranspiration (E_{tot})

Total actual evapotranspiration E_{tot} [mm] is the sum of evaporation (interception E_i, soil E_s and groundwater E_g) and transpiration (shallow U_s and deep U_d root water uptake, transpiration from groundwater Y):

$$E_{tot} = E_i + E_s + E_g + U_s + U_d + Y \tag{43}$$

each described below. It is noted that Canopy interception and transpiration from groundwater are not limited by the total sum being less than potential evaporation – hence total values greater than potential can occur on a given day.

3.3.1 Interception evaporation (E_i)

The evaporation of intercepted rainfall (E_i), following VanDijk (2010) is the widely adopted and evaluated event-based rainfall interception model of Gash (1979), with modifications made later by Gash, Lloyd and Lachaudb (1995) and Van Dijk and Bruijnzeel (2001) to allow application to vegetation with a sparse canopy.

$$E_i(t) = \begin{cases} f_v(t)P_g(t) & if \ P_g(t) < P_{wet}(t) \\ f_v(t)P_{wet}(t) + f_{ER}(t)\left(P_g(t) - P_{wet}(t)\right) & if \ P_g(t) \geq P_{wet}(t) \end{cases} \tag{44}$$

where f_v [-] is the fractional canopy cover (see Section 4 Vegetation Phenology), P_{wet} [mm] is the reference threshold rainfall amount at which the canopy is wet:

$$P_{wet}(t) = -\ln\left(1 - \frac{f_{ER}(t)}{f_v(t)}\right)\frac{S_{veg}(t)}{f_{ER}(t)} \tag{45}$$

For small rainfall events where $P_g(t) < P_{wet}(t)$, all rainfall that falls on the vegetated part of the landscape is assumed to be intercepted. The energy required for evaporation of intercepted water is assumed independent of potential evaporation. It is further assumed that this energy does not reduce the available energy for the remaining evaporative fluxes.

The canopy rainfall storage capacity S_{veg} [mm] given by

$$S_{veg}(t) = s_{leaf} \ LAI(t) \tag{46}$$

where the specific canopy rainfall storage capacity per unit leaf area s_{leaf} [mm] is a HRU specific calibration parameter. LAI is the Leaf Area Index [-], the one-sided greenleaf area per unit ground surface area, that is directly related to f_v (see Section 4).

The ratio of average evaporation rate to average rainfall intensity (during storms) f_{ER} [-] is:

$$f_{ER}(t) = F_{ER0}f_v(t) \tag{47}$$

where the specific ratio of average evaporation rate over average rainfall intensity during storms per unit canopy cover F_{ER0} [-] is a calibration parameter.

3.3.2 Soil evaporation (E_s)

The evaporation from soil E_s [mm] occurs from the unsaturated portion of the grid cell $(1 - f_{sat})$, as a fraction of the potential evaporation (E_0) possible after shallow and deep (E_t) rooted transpiration (described below) have been subtracted:

$$E_s(t) = \left(1 - f_{sat}(t)\right)f_{soil\,E}(t)[E_0(t) - E_t(t)] \tag{48}$$

where the relative soil evaporation $f_{soil\,E}$ [-] is

$$f_{soil\,E}(t) = f_{soil\,E\,max} \min\left(1, \frac{w_0(t)}{w_{0\,\lim E}}\right) \tag{49}$$

and $f_{soil\,E\,max}]$ is the relative soil evaporation when soil water supply is not limiting and $\widehat{w}_{0\,\lim E}$ [-] is the relative top soil water content at which evaporation is reduced.

3.3.3 Evaporation from groundwater (E_g)

The evaporation from groundwater E_g [mm/day] occurs from the saturated portion of the grid cell (f_{sat}), as a fraction of the potential evaporation (E_0) possible after shallow and deep (E_t) rooted transpiration (described below) have been subtracted:

$$E_g(t) = f_{sat}(t)f_{soil\,E\,max}[E_0(t) - E_t(t)] \tag{50}$$

where the same model as the evaporation from soil is used, with the top soil layer saturated $(w_0(t) = 1)$.

3.3.4 Root water uptake from $(E_t = U_s + U_d)$

Total transpiration from plants E_t [mm] in the shallow and deep soil stores is equivalent to the sum of root water uptake from the shallow and deep rooted vegetation. The transpiration fluxes are limited by two factors: a potential transpiration rate $E_{t\,max}$ and a maximum root water uptake U_0. The actual transpiration is then calculated as the lesser of the two and this amount is distributed among the potential transpiration water sources. The overall transpiration rate given by U is used in the estimation of U_s and U_d the shallow and deep rooted vegetation transpiration respectively. As U_s and U_d may be limited by available soil water, an adjusted total transpiration rate is finally recalculated. This final value of E_t is then used to reduce the energy available for direct evaporation.

The maximum root water uptake under ambient conditions U_0 [mm/day] is simply the greater of the maximum root water uptake from the shallow soil store $U_{s\,max}$ [mm/day] and the deep soil store $U_{d\,max}$ [mm/day]:

$$U_0(t) = \max[U_{s\,max}(t), U_{d\,max}(t)] \tag{51}$$

with the maximum root water uptake from the shallow soil store $U_{s\,max}$ [mm/day] given by:

$$U_{s\,max}(t) = U_{s\,MAX} \min\left(1, \frac{w_s(t)}{w_{s\,lim}}\right) \tag{52}$$

with the physiological maximum root water uptake from the shallow soil store $U_{s\,MAX}$ [mm/day] a parameter that is fixed to 6 for both the deep and shallow rooted HRU based on site water use at flux towers (Van Dijk, 2010c). Similarly, the relative shallow soil water content at which transpiration is reduced $w_{s\,lim}$] is fixed to 0.3 for both deep and shallow HRUs.

The maximum root water uptake from the deep soil store $U_{d\,max}$ [mm/day] is given by

$$U_{d\,max}(t) = U_{d\,MAX} \min\left(1, \frac{w_d(t)}{w_{d\,lim}}\right) \tag{53}$$

with the physiological maximum root water uptake from the deep soil store $U_{d\,MAX}$ [mm/day] a parameter for the deep rooted HRU, and fixed to 0 for the shallow rooted HRU (that cannot access the deep soil store). Similarly, the relative deep soil water content at which transpiration is reduced $w_{d\,lim}$], the value is fixed to 0.3 for both deep and shallow HRUs.

The root water uptake U [mm/day] is simply the lesser of the maximum root water uptake under ambient conditions U_0 [mm/day] and the maximum transpiration $E_{t\,max}$ [mm/day]

$$U(t) = \min[U_0(t), E_{t\,max}(t)] \tag{54}$$

where the maximum transpiration $E_{t\,max}$ [mm/day] is given by

$$E_{t\,max}(t) = f_t(t)E_0(t) \tag{55}$$

and the potential transpiration fraction f_t [-] is given by

$$f_t(t) = \frac{1}{1 + \left(\frac{k_\varepsilon(t)}{1 + k_\varepsilon(t)}\right)\frac{g_a(t)}{g_s(t)}} \tag{56}$$

Where g_a [m/s] is aerodynamic conductance, and g_s [m/s] the canopy conductance, and k_ε [-] is a coefficient that determines evaporation efficiency:

$$k_\varepsilon(t) = \Delta(t)/\gamma$$

where Δ [Pa/K] is the slope of the saturation vapour pressure curve, R_n [MJ m^{-2} d^{-1}] net radiation, γ [Pa/K] the psychometric constant.

Aerodynamic conductance (g_a) is given by:

$$g_a(\text{t}) = \frac{0.305\, u_2(t)}{\ln\left(\frac{813}{h_{veg}}-5.45\right)\left(2.3+\ln\left(\frac{813}{h_{veg}}-5.45\right)\right)} \tag{57}$$

where h_{veg} is the height of the vegetation canopy [m]. This equation was derived by Van Dijk (2010c) based on the well-established theory proposed by Thom (1975). The derivation is provided in Appendix B.

The height of the top of the canopy (Figure 13) is derived from the global 1 km lidar estimates of Simard *et al.* (2011) and is assumed to be appropriate only for the deep-rooted HRU. For the shallow-rooted HRU, the vegetation height is optimisable, but is assumed to take a fixed value of 0.5 m. Vegetation height is assumed static throughout the simulation.

Canopy (surface) conductance g_s [m/s] is given by:

$$g_s(\text{t}) = f_v(t)c_{g_s max}V_c \tag{58}$$

where f_v the fractional canopy cover is discussed in Section 4, $c_{g_s max}$ is a coefficient relating vegetation photosynthetic capacity to maximum stomatal conductance (m s⁻¹), and V_c is vegetation photosynthetic capacity index (per unit canopy cover) described in section 3.2 (Energy Balance). $c_{g_s max}$ is currently optimised for both the shallow and deep rooted HRUs, although Van Dijk (2010c) showed that an a priori estimate of 0.03 may be justified.

The root water uptake from the shallow soil store U_s [mm/day] is given by:

$$U_s(t) = \begin{cases} \min\left[S_s(t) - 0.01, \left(\frac{U_{s\,max}(t)}{U_{s\,max}(t)+U_{d\,max}(t)}\right)U(t)\right] & if\ U_0(t) > 0 \\ 0 & if\ U_0(t) \leq 0 \end{cases} \tag{59}$$

The root water uptake from the deep soil store U_d [mm/day] is given by:

$$U_d(t) = \begin{cases} \min\left[S_d(t) - 0.01, \left(\frac{U_{d\,max}(t)}{U_{s\,max}(t)+U_{d\,max}(t)}\right)U(t)\right] & if\ U_0(t) > 0 \\ 0 & if\ U_0(t) \leq 0 \end{cases} \tag{60}$$
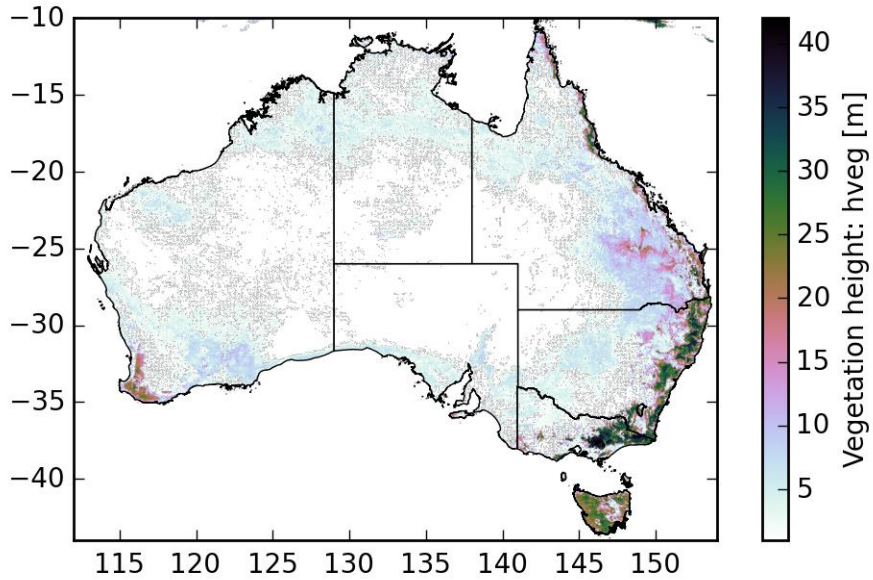
Figure 13. Vegetation height of deep rooted vegetation (h_{veg})

3.3.5 Transpiration from groundwater (Y)

Transpiration from the groundwater store (Y) [mm/day] is given by

$$Y(t) = \begin{cases} \left(f_{E_g}(t) - f_{sat}(t) \right) f_{soil\ E\ max} [E_0(t) - E_t(t)] & if\ f_{sat} < f_{E_g} \\ 0 & if\ f_{sat} \geq f_{E_g} \end{cases} \tag{61}$$

where f_{E_g} [-] is the fraction of the landscape (grid cell) that is accessible for transpiration from groundwater, and f_{sat} [-] is the fraction of the landscape (grid cell) that is saturated.

4 Vegetation Phenology

Vegetation density plays a significant role in the water balance and streamflow generation. Some measure or estimate of vegetation density is therefore crucial for modulating the hydrological processes in AWRA-L.

In the case of AWRA-L leaf biomass M [kg m^{-2}] (directly related to leaf area index LAI and fractional canopy cover f_v – see below) modulates:

- potential evaporation through alteration of albedo (within the energy balance)
- interception through altering the area available for interception and also the rate of interception evaporation
- transpiration through altering canopy conductance

A seasonal vegetation dynamics (or vegetation phenology) model is incorporated into AWRA-L to simulate vegetation cover dynamics in response to water availability. This is done under the assumption that the vegetation takes on the maximum density that could be sustained by the available moisture.

The 'equilibrium' leaf mass is estimated by considering the hypothetical leaf mass M_{eq} that corresponds with a situation in which maximum transpiration rate ($E_{t\,max}$ – Eqn 55) equals maximum root water uptake (U_0 – Eqn 51). The vegetation moves towards this equilibrium state with a prescribed degree of inertia, representative of alternative phenological strategies.

The seasonal vegetation dynamics model is constrained by the mass balance equation. Mass of vegetation M [kg m^{-2}] is given according:

$$M(t + 1) = M(t) + \Delta t M_n(t) \tag{62}$$

where Δt is the length of the time step [1 day], and M_n is the change in leaf biomass at each time step [kg m^{-2} d^{-1}] that moves towards the equilibrium leaf mass (M_{eq}: defined further below) according to:

$$M_n(t) = \begin{cases} \dfrac{M_{eq}(t) - M(t)}{t_{grow}}, & \text{if } M(t) < M_{eq}(t) \\ \dfrac{M_{eq}(t) - M(t)}{t_{senc}}, & \text{if } M(t) \geq M_{eq}(t) \end{cases} \tag{63}$$

where t_{grow} [days] is the characteristic time scale for vegetation growth towards equilibrium, t_{senc} [days] is the characteristic time scale for vegetation senescence towards equilibrium. There is little information available in the literature to estimate t_{grow} and t_{senc} However, they can readily be calibrated to LAI patterns derived from remote sensing. Van Dijk (2010c) notes through visual estimation for around 30 sample locations across Australia, t_{grow} and t_{senc} were both estimated at 50 days for shallow-rooted vegetation, and 90 days for deep-rooted vegetation. However, t_{grow} values of 60 days and 10 days, and t_{senc} values of 1000 days and 150 days have been used subsequently for all version of the AWRA-L model.

This formulation was developed by Van Dijk (2010c) because literature review did not suggest a suitably simple model that predicts water-related vegetation phenology (see review by Arora (2002)). The formulation is based on the assumption that vegetation is able to adjust its leaf biomass at a rate that is independent of the amount of existing leaf biomass and energy or biomass embodied in other plant organs (a strong simplification of the complex physiological processes).

Fractional canopy cover f_v [-], is related to biomass (M) according to the following dimensional conversion firstly to leaf area index LAI [-] (the one-sided greenleaf area per unit ground surface area):

$$LAI(t) = M(t)\, SLA \tag{64}$$

and then:

$$f_v(t) = 1 - \exp\left(-\frac{LAI(t)}{LAI_{ref}}\right) \tag{65}$$

where SLA is the specific leaf area [m^2 kg^{-1}] (the ratio of leaf area to dry mass), and LAI_{ref} is the reference leaf are index [-] corresponding to f_v = 0.632.

As Van Dijk (2010c) explains, the conversion from LAI to f_v is described by the exponential light extinction equation (Monsi and Saeki, 1953) equivalent to Beer's Law which is most commonly used for this purpose. However to be consistent with notation elsewhere in the model, the so-called 'light extinction coefficient' (often symbolised by к) is not used but its inverse value LAI_{ref}, which represents a reference LAI at which fraction cover is 0.632.

Globally reported values of SLA vary by two orders of magnitude, from 0.7 to 71 m^2 kg^{-1} (Wright *et al.*, 2004). Values of 1.5 to 9 m^2 kg^{-1}1 have been found for Australian Eucalypt species (Schulze *et al.*, 2006) with an average value of approximately 3 m^2 kg^{-1}. Fixed values of 10 m^2 kg^{-1} and 3 m^2 kg^{-1} were chosen by Van Dijk (2010c) for shallow and deep rooted vegetation HRUs respectively.

Maximum achievable canopy cover (f_{vmax}) is given, inverting (62), by:

$$f_{vmax} = 1 - \exp\left(-\frac{\max(LAI_{max}, 0.00278)}{LAI_{ref}}\right) \tag{66}$$

where LAI_{max} is the maximum achievable leaf area index [-]. LAI_{max} is derived from a time series of LAI from the Moderate Resolution Imaging Spectroradiometer (MODIS) satellite (Figure 14). At present, the same values of LAI_{max} are used for both HRUs.
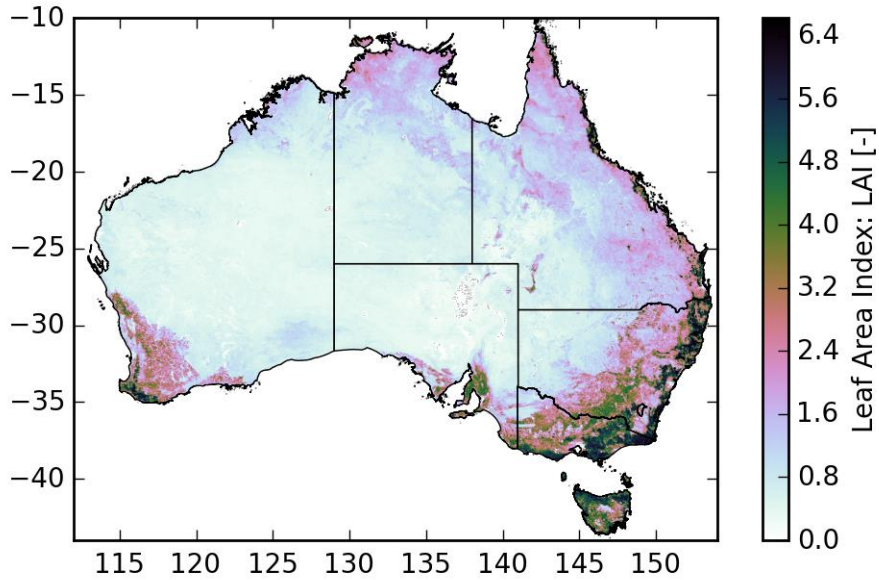
Figure 14. Maximum Leaf Area Index (LAI_{max})

Van Dijk (2010c) derives the equilibrium canopy cover as being given by:

$$f_{veq} = \min\left\{\left(\frac{U_0(t)}{E_0(t) - U_0(t)}\right)\left(\frac{k_\varepsilon(t)}{1 + k_\varepsilon(t)}\right)\frac{g_a(t)}{c_G V_c}, f_{vmax}\right\}$$ (67a)

where the associated equilibrium leaf mass M_{eq} is:

$$M_{eq}(t) = -\frac{LAI_{ref}}{SLA}\ln\left(1 - f_{veq}(t)\right)$$ (67b)

5 Parameterisation

5.1 Parameterisation of AWRA-L v6

AWRA-L v6.0 contains 49 notionally optimisable parameters – see Table 1. Twenty-eight parameters are chosen a priori based through previous experience or according to mapping data – toward reducing the number of parameters to be optimised (and better identifying parameters that the model is sensitive to). The remaining 21 parameters chosen to be free, and are optimised across the continent to maximise a composite objective function combining the performance according to streamflow, ET and soil moisture at a set of 295 unimpaired catchments across Australia (see Figure 15).

The three datasets used in calibration over these catchments across Australia include:

- **Catchment streamflow**: covering the period of 1981-2011. A set of 782 unimpaired catchments with gauged flow records i across Australia were collated by Zhang *et al.* (2013) according to the following criteria: (a) catchment area is greater than 50 km^2, (b) the stream is unregulated (no dams or reservoirs), (c) no major impacts of irrigation and land use, (d) observed record has at least 10 years of data between 1975 and 2011. The catchments (delineated using the Bureau's national catchment Geofabric product: http://www.bom.gov.au/water/geofabric) were collated towards being used in evaluation. The spatial distribution of catchments reserved for calibration and validation of AWRA-L is shown in Figure 15; with regional divisions showing areas of similar climate. Data from 295 catchments covering the period 1/1/1981-30/12/2011 were used in calibration of AWRA-L while 291 catchments not used in calibration are used for validation.

- **Catchment evapotranspiration:** CSIRO MODIS reflectance-based Scaling ET (CMRSET; Guerschman *et al*., 2009) - Satellite retrieval based grid estimates of evapotranspiration covering 2001-2010.

- **Catchment soil moisture:** AMSR-E product (Owe, de Jeu and Holmes, 2008) - Satellite retrieval based grid estimates of soil moisture, covering the period of 2002-2011 have been used.

Various statistics are calculated for each catchment to assess the model's performance during calibration:

Relative bias (B)

$$B_i = \sum_{t=1}^{T} \frac{Q_{mit} - Q_{oit}}{\bar{Q}_{oi}} \qquad (68)$$

Nash-Sutcliffe Efficiency (NSE)

$$NSE_i = 1 - \sum_{t=1}^{T} \frac{(Q_{mit} - Q_{oit})^2}{(Q_{oit} - \bar{Q}_{oit})^2} \tag{69}$$

Pearson's correlation coefficient (r)

$$r_i = \frac{\sum_{t=1}^{T} (Q_{oit} - \bar{Q}_{oi})(Q_{mit} - \bar{Q}_{mi})}{\sqrt{\sum_{t=1}^{T} (Q_{oit} - \bar{Q}_{oi})^2} \sqrt{\sum_{t=1}^{T} (Q_{mit} - \bar{Q}_{mi})^2}} \tag{70}$$

Where Q_{mit} and Q_{oit} represent the modelled simulations and observations respectively for site/catchment i and timestep t for T available observations. $\bar{Q}_{oi}$ and $\bar{Q}_{mi}$ are the mean of the observations and modelled outputs respectively over all timesteps.

The following streamflow objective function is evaluated for each catchment simulation (as derived by Viney et al., 2009):

$$F_s = NSE_d - 5 \mid \ln(1 + B) \mid^{2.5} \tag{71}$$

where NSE_d is the daily Nash-Sutcliffe Efficiency (Eq. 69) and B is relative bias (B). Daily soil moisture correlation (r_{sm}) and monthly evapotranspiration (r_{et}) (defined in Eq. 58) are also used for each catchment according to the weighted function:

$$F = 0.7 * F_s + 0.15 * r_{sm} + 0.15 * r_{et} \tag{72}$$

Finally, the national calibration of AWRA-L maximises the grand objective function:

$$grandF = mean(F_{25\%}, F_{50\%}, F_{75\%}, F_{100\%}) \tag{73}$$

where $F_{X\%}$ is the Xth ranked site percentile F value. This objective function aims to get an adequate fit over a wide range of sites, but also to exclude very poor fitting areas (i.e. those below the 25%).

For further details of calibration, evaluation of model performance and a-priori specification of model parameters see Viney *et al.* (2015), Frost and Wright (2018b, 2018a) and Van Dijk (2010c).

Table 1. AWRA-L v5 and v6 parameter values. Values that apply to either the deep or shallow rooted HRU (or both) are provided. Values that are optimised are shown in bold.

Symbol	Definition	AWRA Lv5 Deep	AWRA Lv5 Shallow	AWRA-L v6 Deep	AWRA-L v6 Shallow	Unit
α_d	Dry soil albedo	0.26	0.26	0.26	0.26	-
α_w	Wet soil albedo	0.16	0.16	0.16	0.16	-
c_G	Conversion coefficient from vegetation photosynthetic capacity index to maximum stomatal conductance	**0.0320**	**0.0237**	**0.021248**	**0.032094**	m/s
f_{ER}	Ratio of average evaporation rate over average rainfall intensity during storms per unit canopy cover	**0.0736**	0.5	**0.0736**	0.5	-
F_{smax}	Soil evaporation scaling factor when soil water supply is not limiting evaporation	**0.2275**	**0.9297**	**0.585005**	**0.999608**	-
h_{veg}	Height of vegetation canopy	Grid	0.5	Grid	0.5	m
LAI_{ref}	Reference leaf area index (at which fv = 0.63)	2.5	1.4	2.5	1.4	-
SLA	Specific leaf area	3	10			m²/kg
s_l	Specific canopy rainfall storage capacity per unit leaf area	**0.0946**	**0.0427**	**0.067438**	**0.29277**	mm
t_{grow}	Characteristic time scale for vegetation growth towards equilibrium	1000	150	1000	150	days
t_{senc}	Characteristic time scale for vegetation senescence towards equilibrium	60	10	60	10	days
U_{s0}	Shallow soil Max. root water uptake rates	0	6	0	6	mm/d
U_{d0}	Deep soil Max. root water uptake rates	**7.1364**	0	**11.56989**	**0**	mm/d
V_c	Vegetation photosynthetic capacity index per unit canopy cover	0.35	0.65	0.35	0.65	-
w_{0lim}	Relative top soil water content at which evaporation is reduced	0.85	0.85	0.85	0.85	-
w_{slim}	Water-limiting relative water content in shallow store	0.3	0.3	0.3	0.3	-
w_{dlim}	Water-limiting relative water content in deep store	0.3	0.3	0.3	0.3	-
D_R	Rooting depth	6	1	6	1	m
$K_{gw\ scale}$	Multiplier on the raster input of K_{gw}	**0.5022**		**0.93908135**		-
K_{rint}	Intercept coefficient for calculating routing coefficient K_r	**0.1577**		**0.16542047**		-
K_{rscale}	Scale coefficient for calculating routing coefficient K_r	**0.0508**		**0.04855041**		-
k_β	Coefficient on the mapped slope for interflow	**0.9518**		**0.43879647**		-
k_ζ	K_{sat} ratio coefficient across soil horizons for interflow	**0.0741**		**0.66159026**		-
$K_{0satscale}$	Saturated hydraulic conductivity scale in top layer	**2.8728**		**3.89200702**		-
$K_{ssatscale}$	Saturated hydraulic conductivity scale in shallow layer	**0.0202**		**0.05234894**		-
$K_{dsatscale}$	Saturated hydraulic conductivity scale in deep layer	**0.0100**		**0.0122021**		-
n_{scale}	Scale for effective porosity	**0.0552**		**0.04253378**		-
$P_{refscale}$	Multiplier on the raster input of P_{ref}	**1.8153**		**2.56420087**		-
$S_{0maxscale}$	Scale for maximum water storage in the surface layer	**2.9958**		**2.80487914**		-
$S_{smaxscale}$	Scale for maximum water storage in the shallow layer	**2.4333**		**1.99322065**		-
$S_{dmaxscale}$	Scale for maximum water storage in the deep layer	**0.7951**		**0.88436116**		-
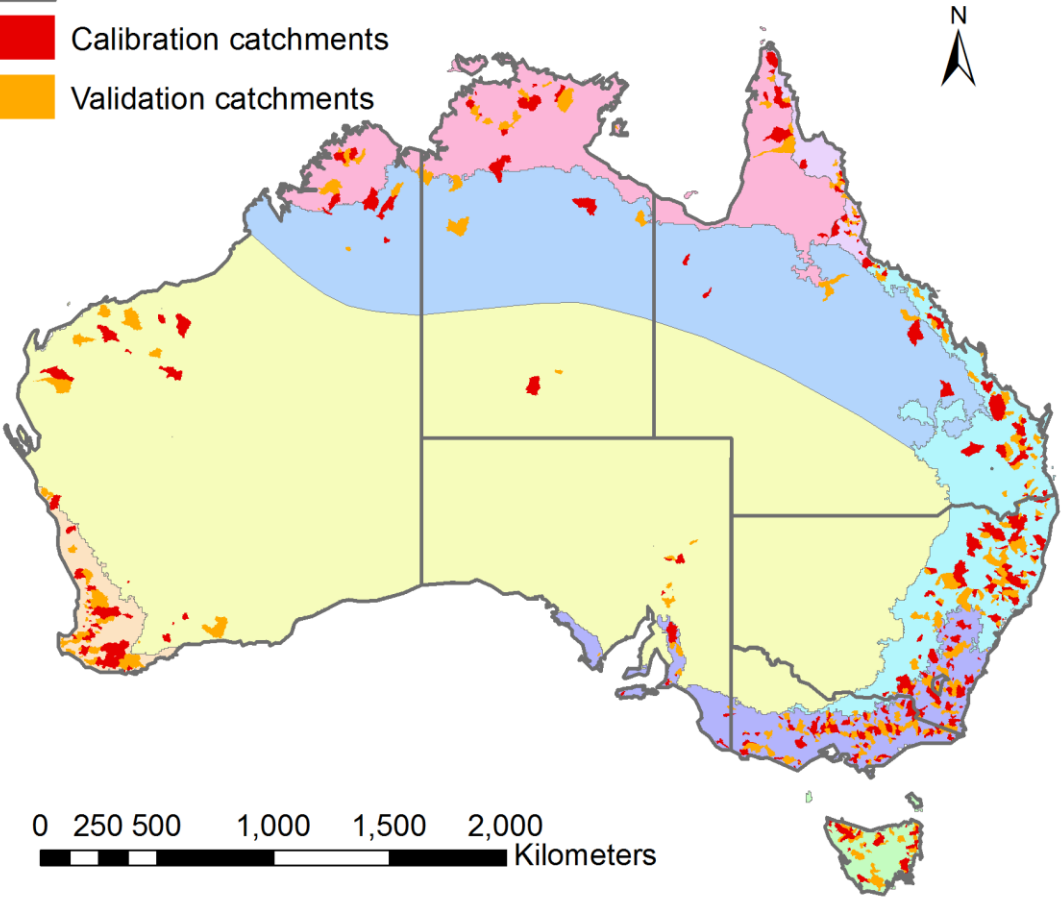
Figure 15. Location of unimpaired catchments used for model evaluation with climate zones overlain.

5.2 Differences between AWRA-L v5 and AWRA-L v6

Various changes have been implemented within version 6 based on experimentation described within Frost and Wright (2018b). This section summarises those changes.

5.2.1 Climate inputs

Solar radiation: updated input forcing data with improved site based bias correction (Ian Grant, Bureau of Meteorology, *pers comm*) covering 1990 onwards; with a daily varying climatology used when there is missing data based on the period 1990-2017.

Wind: u_2 Wind speed at a height of 2 m [m/s]:

- Removal of calculation of effective daytime wind speed introduced by Van Dijk (Eqn [3-12], 2010) introduced to account for diurnal fluctuations in wind:

$$u_2 = \left[\frac{1 - (1 - f_{day})0.25}{f_{day}}\right] WINDSPEED$$

According to the fraction of daylight hours (f_{day}). This had an effect of increasing windspeed seasonally. AWRA-L v6 uses :

$$u_2 = WINDSPEED;$$

which then is reduced comparatively to AWRA-L v5, flowing on to reduced potential evapotranspiration according to Equation (31), all other things being equal.

- Direct use of the daily varying interpolated daily wind run data (McVicar et al., 2008) rather than using a constant climatology based on 1975-2017. This causes greater variability of outputs from 1975 onwards; where climatology is used prior to 1975.

5.2.2 Updated static spatial inputs:

Fraction deep rooted vegetation within each grid cell (as described in 1.3.3)**:** The fraction of tree cover within each grid cell (denoted as f_{tree}) is used to apportion the grid cell area to each of the two Hydrological Response Units used within AWRA. It is based in version 6 on the Advanced Very High Resolution radiometer (AVHRR) satellite derived fractions of persistent and recurrent photosynthetically active absorbed radiation (fPAR) (Donohue, Roderick and McVicar, 2008) version 5; from 0.05 degree (5km data) covering 1981-2011 available through:
https://doi.org/10.4225/08/50FE0CBE0DD06

Hypsometric curves (see 2.1.3) is the cumulative distribution of elevation within an AWRA-L grid cell and is used for conversion from groundwater storage to head relative to the lowest point in the cell. The head level determines the fraction of saturated groundwater (which affects the amount of saturated excess overland flow) and the fraction of groundwater available for transpiration. In AWRA v6, this is based on a finer scale SRTM based DEM (1 second, previous versions used a 9 second DEM). See the DEM_S in https://data.gov.au/dataset/srtm-derived-1-second-digital-elevation-models-version-1-0.

Soil storage and drainage properties (see section 2.1.2) : $K_{xsatPEDO}$ is the saturated hydraulic conductivities of three soil layers (where: $x = 0$: top 0-10cm, $x = s$: shallow 10-100cm, and $x = d$: deep 100-600cm) derived from the pedotransfer functions of Dane and Puckett (1994) applied to the continental scale mapping of clay content from the Terrestrial Ecosystem Research Network (TERN) Soil and Landscape Grids of Australia (http://tern.org.au/Soil-and-Landscape-Grid-of-Australia-pg17731.html). S_{xAWC} is the (proportional) available water holding capacity of the soil layers and was derived from clay content using pedotransfer functions within Minasny *et al.* (1999). This replaces information used in version 5 derived from ASRIS Level 4 (Johnston *et al.*, 2003). The rationale and approach for deriving these surfaces is described in Vaze *et al.* (2018).

5.2.3   Soil drainage equations

The effective saturated conductivity for the top and shallow layers were altered, changing the soil drainage behaviour (see section 2.1.2). The geometric averaging of saturated conductivity of the layer being considered and the layer below in the drainage equation (11) and (12) was removed. For example, K_{0sat}, the average saturated conductivity of the top (0-10cm) layer drainage rather than $\sqrt{K_{0sat}K_{ssat}}$ in the drainage equation (11) in Frost et al. (2016): $D_0(t) + Q_{I0}(t) = \sqrt{K_{0sat}K_{ssat}} \left(\frac{S_0(t)}{S_{0max}}\right)^2$. This was chosen so that the saturated conductivity being used reflects the drainage layer that it applied to and not the layer below. This tends to make the effective saturated conductivity higher for any given layer.

5.2.4   Calibration Objective Function

The objective function used in AWRA-L v6 calibration (see section 5.1) was different to that used in v5. The following site based streamflow objective function, including a monthly Nash-Sutcliffe Efficiency NSE_m was used in v5 :

$$F_s = (NSE_d + NSE_m)/2 - 5 \mid \ln(1 + B) \mid^{2.5}$$

The updated objective function (Eqn. 71) did not use the NSE_m term and was chosen based on performance according to a range of soil moisture, evapotranspiration,

streamflow and groundwater observations nationally – see Frost and Wright (2018b). The results show that AWRA-L v6 has better daily NSE characteristics than v5, although monthly NSE statistics aren't as good as they could be if that component was used in calibration. For detailed experimentation and validation details see Frost and Wright (2018b, 2018a).

References

Allen, R. G. *et al.* (1998) 'Crop evapotranspiration: Guidelines for computing crop requirements', *Irrigation and Drainage Paper No. 56, FAO*, (56), p. 300. doi: 10.1016/j.eja.2010.12.001.

Arora, V. (2002) 'Modeling vegetation as a dynamic component in soil-vegetation-atmosphere transfer schemes and hydrological models', *Reviews of Geophysics*, 40(2), pp. 1–26. doi: 10.1029/2001RG000103.

Brunt, D. (1932) 'Notes on radiation in the atmosphere. I', *Quarterly Journal of the Royal Meteorological Society*, 58(247), pp. 389–420. doi: 10.1002/qj.49705824704.

Brutsaert, W. (1975) 'On a derivable formula for long-wave radiation from clear skies', *Water Resources Research*, 11(5), pp. 742–744. doi: 10.1029/WR011i005p00742.

Dane, J. H. and Puckett, W. (1994) 'Field soil hydraulic properties based on physical and mineralogical information', in al., Mt. van G. et (ed.) *International Workshop on Indirect Methods for Estimating the Hydraulic Properties of Unsaturated Soils*. Riverside, CA: University of California, pp. 389–403.

Dong, A. *et al.* (1992) 'Estimation of Daytime Net Radiation Over Well Watered Grass', *Journal of Irrigation and Drainage Engineering*, 118(3), pp. 466–479. doi: 10.1061/(ASCE)0733-9437(1992)118:3(466).

Donohue, R. J., Mcvicar, T. R. and Roderick, M. L. (2009) *Generating Australian potential evaporation data suitable for assessing the dynamics in evaporative demand within a changing climate*. CSIRO: Water for a Healthy Country National Research Flagship.

Donohue, R. J., Roderick, M. L. and McVicar, T. R. (2008) 'Deriving consistent long-term vegetation information from AVHRR reflectance data using a cover-triangle-based framework', *Remote Sensing of Environment*, 112(6), pp. 2938–2949. doi: http://dx.doi.org/10.1016/j.rse.2008.02.008.

Duffie, J. A. and Beckman, W. A. (2013) *Solar Engineering of Thermal Processes Solar Engineering*. 4th edn. Hoboken, New Jersey: Wiley.

Elmahdi, A. *et al.* (2015) 'Australian Water Resources Assessment Modelling System (AWRAMS)-informing water resources assessment and national water accounting', *36th Hydrology and Water Resources Symposium: The art and science of water. Barton, ACT: Engineers Australia*, pp. 979–986.

Fröhlich, C. and Brusa, R. W. (1981) 'Solar radiation and its variation in time', *Solar Physics*, 74, pp. 209–215. doi: 10.1017/CBO9781107415324.004.

Frost, A. J. and Wright, D. P. (2018a) *Evaluation of the Australian Landscape Water Balance model (AWRA-L v6): Comparison of AWRA-L v6 against Observed Hydrological Data and Peer Models*. Technical report. Bureau of Meteorology.

Frost, A. J. and Wright, D. P. (2018b) 'The Australian Water Resource Assessment Landscape model – AWRA-L: improved performance and regional calibration', in *Proceedings from HWRS2018: Hydrology and Water Resources Symposium, Melbourne*.

Gash, J. H. C. (1979) 'An analytical model of rainfall interception by forests', *Quarterly Journal of the Royal Meteorological Society*, 105(443), pp. 43–55. doi: 10.1002/qj.49710544304.

Gash, J. H. C., Lloyd, C. R. and Lachaudb, G. (1995) 'Estimating sparse forest rainfall interception with an analytical model', *Journal of Hydrology*, 170(95), pp. 79–86. doi: 10.1016/0022-1694(95)02697-N.

Grant, I. *et al.* (2008) 'Meteorological and remotely sensed datasets for hydrological modelling: a contribution to the Australian Water Availability Project', in *Proceedings of the Catchment-scale Hydrological Modelling & Data Assimilation (CAHMDA-3) International Workshop on Hydrological Prediction: Modelling, Observation and Data Assimilation, January 9 2008–January 11 2008*.

Guerschman, J. P. *et al.* (2009) 'Scaling of potential evapotranspiration with MODIS data reproduces flux observations and catchment water balance observations across Australia', *Journal of Hydrology*, 369(1–2), pp. 107–119. Available at: http://www.sciencedirect.com/science/article/B6V6C-4VMGV01-1/2/45782648e306eb0ef4352384e77d228a.

Hafeez, M. *et al.* (2015) 'The Bureau's Operational AWRA Modelling System in the context of Australian landscape and hydrological model products', *36th Hydrology and Water Resources Symposium*. Hobart, Australia: Engineers Australia, (December).

Iqbal, M. (1983) *An Introduction to Solar Radiation*.

Jensen, M. E., Wright, J. L. and Pratt, B. J. (1971) 'Estimating Soil Moisture Depletion from Climate, Crop and Soil Data', *Transaction of the ASAE*, 14(5), pp. 954–959.

Johnston, R. M. *et al.* (2003) 'ASRIS: the database', *Soil Research*, 41(6), pp. 1021–1036. doi: http://dx.doi.org/10.1071/SR02033.

Jones, D. A., Wang, W. and Fawcett, R. (2009) 'High-quality spatial climate data-sets for Australia', *Australian Meteorological and Oceanographic Journal*, 58, pp. 233–248.

Liu, B. Y. H. and Jordan, R. C. (1960) 'The interrelationship and characteristic distribution of direct, diffuse and total solar radiation', *Solar Energy*, 4(3), pp. 1–19. doi: 10.1016/0038-092X(60)90062-1.

McVicar, T. R. *et al.* (2008) 'Wind speed climatology and trends for Australia, 1975-2006: Capturing the stilling phenomenon and comparison with near-surface reanalysis output', *Geophysical Research Letters*, 35(L20403). doi: 10.1029/2008GL035627.

Minasny, B. and McBratney, A. B. (2000) 'Evaluation and development of hydraulic conductivity pedotransfer functions for Australian soil', *Soil Research*, 38(4), pp. 905–

926. Available at: https://doi.org/10.1071/SR99110.

Minasny, B., McBratney, A. B. and Bristow, K. L. (1999) 'Comparison of different approaches to the development of pedotransfer functions for water-retention curves', *Geoderma*, 93(3), pp. 225–253. doi: https://doi.org/10.1016/S0016-7061(99)00061-0.

Monsi, M. and Saeki, T. (1953) 'Über den Lichtfaktor in den Pflanzengesellschaften und seine Bedeutung für die Stoffproduktion', *Japanese Journal of Botany*, 14, pp. 22–52. doi: 10.1093/aob/mci052.

Owe, M., de Jeu, R. and Holmes, T. (2008) 'Multisensor historical climatology of satellite-derived global land surface moisture', *Journal of Geophysical Research: Earth Surface*, 113(F1), p. F01002. doi: 10.1029/2007jf000769.

Peeters, L. J. M. *et al.* (2013) 'Conceptual evaluation of continental land-surface model behaviour', *Environmental Modelling & Software*, 43(0), pp. 49–59. doi: http://dx.doi.org/10.1016/j.envsoft.2013.01.007.

Penman, H. L. (1948) 'Natural Evporation from Open Water, Bare Soil and Grass', *The Royal Society*, 193(1032), pp. 120–145. doi: 10.1098/rspa.1948.0037.

Raupach, M. R. *et al.* (2008) *Australian Water Availability Project (AWAP) - CSIRO Marine and Atmospheric Research Component: Final Report for Phase 3*. Caberra, Australia: CSIRO Marine and Atmospheric Research.

Roderick, M. L. (1999) 'Estimating the diffuse component from daily and monthly measurements of global radiation', *Agricultural and Forest Meteorology*, 95(3), pp. 169–185. doi: 10.1016/S0168-1923(99)00028-3.

Schulze, E. D. *et al.* (2006) 'Species differences in carbon isotope ratios, specific leaf area and nitrogen concentrations in leaves of Eucalyptus growing in a common garden compared with along an aridity gradient', *Physiologia Plantarum*, 127(3), pp. 434–444. doi: 10.1111/j.1399-3054.2006.00682.x.

Shuttleworth, W. J. (1992) 'Chapter 4. Evaporation', in Maidment, D. R. (ed.) *'Handbook of Hydrology'*, p. 4.1-4.53.

Simard, M. *et al.* (2011) 'Mapping forest canopy height globally with spaceborne lidar', *Journal of Geophysical Research: Biogeosciences*, 116(G4), p. G04021. doi: 10.1029/2011jg001708.

Spencer, J. W. (1971) 'Fourier series representation of the position of the Sun', *Search*, 2(5), p. 172.

Thom, A. . (1975) '3. Momentum, Mass and Heat Exchange of Plant Communities', in *Vegetation and the atmosphere: principles*, p. 57.

Van Dijk, A. I. J. M. (2010a) 'Climate and terrain factors explaining streamflow response and recession in Australian catchments', *Hydrology and Earth System Sciences*. Copernicus GmbH, 14(1), pp. 159–169. doi: 10.5194/hess-14-159-2010.

Van Dijk, A. I. J. M. (2010b) 'Selection of an appropriately simple storm runoff model', *Hydrology and Earth System Sciences.* Copernicus GmbH, 14(3), pp. 447–458. doi: 10.5194/hess-14-447-2010.

Van Dijk, A. I. J. M. (2010c) *The Australian Water Resources Assessment System. Technical Report 3. Landscape Model (version 0.5) Technical Description.* CSIRO: Water for a Healthy Country National Research Flagship.

Van Dijk, A. I. J. M. and Bruijnzeel, L. A. (2001) 'Modelling rainfall interception by vegetation of variable density using an adapted analytical model. Part 1. Model description', *Journal of Hydrology*, 247(3–4), pp. 230–238. doi: 10.1016/S0022-1694(01)00392-4.

Vaze, J. *et al.* (2013) 'The Australian Water Resource Assessment System (AWRA)', in *Proceedings of the 20th International Congress on Modelling and Simulation.* Adelaide, Australia.

Vaze, J. *et al.* (2018) *AWRA-L input spatial layers at 1 km and 5 km resolutions for the Australian continent - Source data and comparison between 1 km and 5 km resolutions.*

Viney, N. *et al.* (2015) *AWRA-L v5.0: technical description of model algorithms and inputs.* CSIRO, Australia.

Viney, N. R. *et al.* (2014) 'The AWRA modelling system', *Hydrology and Water Resources Symposium 2014.* Perth: Engineers Australia, pp. 1018–1025. Available at: http://search.informit.com.au/documentSummary;dn=388600432195626;res=IELENG.

Wright, I. J. *et al.* (2004) 'The worldwide leaf economics spectrum', *Nature*, 428, pp. 821–827. doi: 10.1038/nature02403.

Wright, J. L. (1982) 'New Evapotranspiration Crop Coefficients', *Journal of the Irrigation and Drainage Division*, 108(1), pp. 57–74.

Wright, J. L. and Jensen, M. E. (1972) 'Peak Water Requirements of Crops in Southern Idaho', *Journal of the Irrigation and Drainage Division*, 98(IR2), pp. 193–201.

Zhang, Y. Q. *et al.* (2013) *Collation of streamflow and catchment attribute dataset for 780 unregulated Australian catchments.* CSIRO: Water for a Healthy Country National Research Flagship.

Appendices

Appendix A: Table of model variables

Appendix B: Downward longwave radiation derivation

Appendix A: Table of model variables

Table 2. List of variable names used in this document and the corresponding variables used in the model code. Units are those given in this document.

Document	Model code	Description
α	alb	Surface albedo (dimensionless)
α_{dry}	alb_dry	Dry soil albedo (dimensionless)
α_s	alb_soil	Albedo of soil surface (dimensionless)
α_v	alb_veg	Albedo of vegetated surfaces (dimensionless)
α_{wet}	alb_wet	Wet soil albedo (dimensionless)
β	slope	Slope of the land surface (percent)
γ	gamma	Psychrometric constant (Pa K^{-1})
Δ	delta	Slope of the saturation vapour pressure curve (Pa K^{-1})
δ	DELTA	Solar declination (radians)
λ	lambda	Latent heat of vaporisation (MJ kg^{-1})
λ_d	Dd	Surface water drainage density (m^{-1})
ρ_0	Rh_0s	Partitioning factor for vertical and lateral drainage from the surface soil layer (dimensionless)
ρ_s	Rh_sd	Partitioning factor for vertical and lateral drainage from the shallow soil layer (dimensionless)
σ	StefBolz	Stefan-Boltzmann constant (MJ m^{-2} d^{-1} K^{-4})
ϕ	latitude	Latitude (radians), and is negative in the southern hemisphere
ω	PI	Sunset hour angle (radians)
$c_{g_s max}$	cGsmax	Coefficient relating vegetation photosynthetic capacity to maximum stomatal conductance (m s^{-1})
D_0	D0	Vertical drainage from the bottom of the surface soil layer (mm)
D_d	Dd	Vertical drainage from the bottom of the deep soil layer (mm)
D_R	RD	Rooting depth (m)
D_s	Ds	Vertical drainage from the bottom of the shallow soil layer (mm)
DOY	DayOfYear	Day of the year (d)
d_0	—	Depth of the top soil layer (mm)
d_d	—	Depth of the deep soil layer (mm)
d_s	—	Depth of the shallow soil layer (mm)
d_u	—	Depth of the unconfined aquifer (m)
E_0	E0	Potential evaporation (mm d^{-1})
$\overline{E^*}$	meanpet	Long term mean daily potential evaporation (mm d^{-1})
E_s	Es	Evaporation flux from the surface soil store (mm d^{-1})
E_g	Eg	Evaporation flux from the groundwater store (mm d^{-1})
E_i	Ei	Evaporation flux from canopy interception (mm d^{-1})
E_t	Et	Actual total transpiration flux (mm d^{-1})
$E_{t\,max}$	Etmax	Potential transpiration rate (mm d^{-1})
E_{tot}	Etot	Total evapotranspiration (mm d^{-1})
F_{ER0}	ER_frac_ref	Specific ratio of the mean evaporation rate and the mean rainfall intensity during storms
$f_{soil\,E}$	fsoile	Relative soil evaporation
$f_{soil\,E\,max}$	fsoilemax	Soil evaporation scaling factor corresponding to unlimited soil water supply (dimensionless)
f_{Eg}	fEgt	Fraction of the grid cell that is accessible for transpiration from groundwater (dimensionless)
f_{er}	fer	ratio of average evaporation rate to average rainfall intensity (during storms)
f_{sat}	fsat	Fraction of the grid cell that is saturated at the surface (dimensionless)
f_{tree}	f_tree	Fraction of tree cover within each grid cell (dimensionless)
f_v	fveg	Fractional canopy cover (dimensionless)
f_{veq}	fveq	Equilibrium canopy cover (dimensionless)
$fPAR$	—	Photosynthetically-active radiation (dimensionless)
g_a	ga	Aerodynamic conductance (m s^{-1})

g_s	gs	Canopy conductance (m s^{-1})
H_b	—	Drainage base – the lowest topographic point within the grid cell (m)
h	—	Elevation of a point on the hypsometric curve (m)
h_u	—	Elevation change along the flow path (m)
h_{veg}	hveg	Vegetation height (m)
I	I	Infiltration (mm)
K_{0sat}	K0sat	Saturated hydraulic conductivity of surface soil layer (mm d^{-1})
$K_{0satscale}$	K0sat_scale	Scaling factor for hydraulic conductivity of surface soil layer(dimensionless)
$K_{0satPEDO}$	K0sat_grid	Saturated hydraulic conductivity of surface soil layer from pedtransfer(mm d^{-1})
K_d	Rgeff	Daily downwelling shortwave (solar) radiation (MJ m^{-2} d^{-1})
K_{d0}	RadClearSky	Expected downwelling shortwave radiation on a cloudless day (MJ m^{-2} d^{1})
K_{dsat}	Kdsat	Saturated hydraulic conductivity of deep soil layer (mm d^{-1})
$K_{dsatPEDO}$	Kdsat_grid	Saturated hydraulic conductivity of deep soil layer from pedotransfer (mmd^{-1})
$K_{dsatscale}$	Kdsat_scale	Scaling factor for hydraulic conductivity of deep soil layer (dimensionless)
K_{gmap}	K_gw_grid	Groundwater drainage coefficient obtained from continental mapping (d^{-1})
K_{gscale}	K_gw_scale	Scaling factor for groundwater drainage coefficient (dimensionless)
K_g	K_gw	Groundwater drainage coefficient (d^{-1})
K_r	K_rout	Rate coefficient controlling discharge to stream (dimensionless)
K_{rint}	Krout_int	Intercept coefficient for calculating K_r (dimensionless)
K_{rscale}	K_rout_scale	Scale coefficient for calculating K_r (d mm^{-1})
K_{ssat}	Kssat	Saturated hydraulic conductivity of shallow soil layer (mm d^{-1})
$K_{ssatPEDO}$	Kssat_grid	Saturated hydraulic conductivity of shallow soil layer from pedotransfer (mm d^{-1})
$K_{ssatscale}$	Kssat_scale	Scaling factor for hydraulic conductivity of shallow soil layer (dimensionless)
K_u	—	Daily upwelling shortwave radiation (MJ m^{-2} d^{-1})
k_β	slope_coeff	Scaling factor for slope (dimensionless)
k_u	—	Hydraulic conductivity of the unconfined aquifer (m d^{-1})
k_ζ	Kr_coeff	Scaling factor for ratio of saturated hydraulic conductivity (dimensionless)
LAI	LAI	Leaf area index (LAI) (dimensionless)
LAI_{max}	LAImax	Maximum achievable LAI value (dimensionless)
LAI_{ref}	LAIref	Reference LAI value corresponding to f_v = 0.63 (dimensionless)
L_d	RLin	Daily downwelling longwave radiation (MJ m^{-2} d^{-1})
L_u	RLout	Daily upwelling longwave radiation (MJ m^{-2} d^{-1})
M	Mleaf	Leaf biomass (kg m^{-2})
M_{eq}	—	Equilibrium leaf biomass (kg m^{-2})
M_n	Mleafnet	Change in leaf biomass at each time step (kg m^{-2} d^{-1})
n	ne	Effective porosity (dimensionless)
n_{map}	—	Effective porosity obtained from continental mapping (dimensionless)
n_{scale}	ne_scale	Scaling factor for effective porosity (dimensionless)
P_{wet}	Pwet	Reference threshold precipitation amount (mm)
P_g	Pg	Gross precipitation (mm)
P_n	Pn	Net precipitation – precipitation minus interception (mm)
P_{ref}	PrefR	Reference value for precipitation (mm)
P_{refmap}	—	Mapped reference value for precipitation (mm) prior to scaling
$P_{refscale}$	Pref_gridscale	Scaling factor for reference precipitation (dimensionless)
p_e	pe	Actual vapour pressure (Pa)
p_{es}	pes	Saturation vapour pressure (Pa)
Q_g	Qg	Groundwater discharge to the surface water (mm)
Q_h	Rhof	Infiltration-excess runoff component (mm)

Q_{IF}	QIF	Interflow (mm)
Q_{I0}	IF0	Interflow draining laterally from the surface soil layer (mm)
Q_{Is}	IFs	Interflow draining laterally from the shallow soil layer (mm)
Q_R	QR	Surface runoff (mm)
Q_s	Rsof	Saturation-excess runoff component (mm)
Q_t	Qtot	Total discharge to stream (mm)
R_n	Rneff	Daily net radiation (MJ m^{-2} d^{-1})
SLA	SLA	Specific leaf area (m^2 kg^{-1})
S_0	S0	Water storage in the surface soil layer (mm)
S_{0AWC}	S0fracAWC_grid	Available water holding capacity in the surface soil (dimensionless)
S_{0max}	S0max	Maximum storage of the surface soil layer (mm)
$S_{0maxscale}$	S0max_scale	Scaling parameter for maximum storage of the surface soil layer(dimensionless)
S_d	Sd	Water content of the deep soil store (mm)
S_{dmax}	Sdmax	Maximum storage of the deep soil layer (mm)
$S_{dmaxscale}$	Sdmax_scale	Scaling parameter for maximum storage of the deep soil layer(dimensionless)
S_g	Sg	Groundwater storage in the unconfined aquifer (mm)
S_r	Sr	Volume of water in the surface water store (mm)
S_s	Ss	Water content of the shallow soil store (mm)
S_{sAWC}	SsfracAWC_grid	Available water holding capacity in the shallow soil (dimensionless)
S_{smax}	Ssmax	Maximum storage of the shallow soil layer (mm)
$S_{smaxscale}$	Ssmax_scale	Scaling parameter for maximum storage of the shallow soil layer (dimensionless)
S_{leaf}	S_sls	Specific canopy rainfall storage per unit leaf area (mm)
S_{veg}	sveg	Canopy rainfall storage capacity (mm)
T	-	Surface temperature (K)
T_a	Ta	Daily mean temperature (°C)
T_{max}	Tmax	Maximum air temperature (°C)
T_{min}	Tmin	Minimum air temperature (°C)
t	—	Time step (d)
Δt	—	Length of the time step (d)
t_{grow}	Tgrow	Characteristic time scale for vegetation growth towards equilibrium (d)
t_{senc}	Tsenc	Characteristic time scale for vegetation senescence towards equilibrium(d)
U_0	U0	Maximum root water uptake (mm d^{-1})
U_d	Ud	Root water uptake (transpiration) from the deep soil store (mm d^{-1})
U_{dMAX}	Ud0	Maximum possible root water uptake from the deep soil store (mm d^{-1})
U_{dmax}	Udmax	Maximum root water uptake from the deep soil store at prevailing moisture content (mm d^{-1})
U_s	Us	Root water uptake (transpiration) from the shallow soil store (mm d^{-1})
U_{sMAX}	Us0	Maximum possible root water uptake from the shallow soil store (mm d^{-1})
U_{smax}	Usmax	Maximum root water uptake from the shallow soil store at prevailing moisture content (mm d^{-1})
u_2	u2	Wind speed at a height of 2 m (m s^{-1})
V_c	Vc	Vegetation photosynthetic capacity per unit canopy cover
w_0	w0	Relative soil moisture content of the top soil layer (dimensionless)
w_{0limE}	w0limE	Limiting the value of w_0 at which evaporation is reduced (dimensionless)
w_{0ref}	w0ref_alb	Reference value of w_0 that determines the rate of albedo decrease with wetness (dimensionless)
W_d	wd	Relative water content of the deep soil store (dimensionless)
W_{dlim}	wdlimU	Water-limiting relative water content of the deep soil store(dimensionless)
w_s	ws	Relative water content of the shallow soil store(dimensionless)
w_{slim}	wslimU	Water-limiting relative water content of the shallow soil store(dimensionless)
Y	Y	Root water uptake (transpiration) from the groundwater store (mm d^{-1})

Appendix B: Downward longwave radiation derivation

The downward longwave radiation L_d [W/m²] is derived from the net incoming longwave radiation $R_{ln\,in}$ [W/m²] and the upward longwave radiation L_u [W/m²] as (Shuttleworth, 1992)

$$R_{ln\,in}(t) = L_d(t) - L_u(t) \tag{74}$$

with net outgoing longwave radiation $R_{ln\,out}$ [W/m²], a negative flux (as $L_u > L_d$), given by

$$R_{ln\,out}(t) = -R_{ln\,in}(t) \tag{75}$$

Therefore, downward longwave radiation L_d [W/m²] is given as

$$L_d(t) = L_u(t) - R_{ln\,out}(t) \tag{76}$$

with net outgoing longwave radiation $R_{ln\,out}$ [W/m²] given by (Jensen, Wright and Pratt, 1971; Wright and Jensen, 1972; Wright, 1982; Shuttleworth, 1992; Allen *et al.*, 1998)

$$R_{ln\,out}(t) = f(t)R_{ln0\,out}(t) \tag{77}$$

where the net outgoing longwave radiation for a clear sky $R_{ln0\,out}$ [W/m²] is given by (Brunt, 1932; Jensen, Wright and Pratt, 1971; Wright and Jensen, 1972; Wright, 1982; Allen *et al.*, 1998)

$$R_{ln0\,out}(t) = \left(1 - \varepsilon_{a0}(t)\right)\sigma(T_a(t) + 273.15)^4 \tag{78}$$

Where the surface emissivity ε is assumed 1, and $\boldsymbol{\varepsilon_{a0}}$ [-] is the atmospheric emissivity for a clear sky (Brutsaert, 1975) calculated from actual vapour pressure e_a [mbar] and daytime air temperature [°K]

$$\varepsilon_{a0}(t) = 1.24\left(\frac{e_a(t)}{T_a(t)}\right)^{\frac{1}{7}} \tag{79}$$

Or equivalently (with some truncation) after the units of vapour pressure e_a [Pa] and daytime air temperature [°C] have been changed.

$$\varepsilon_{a0}(t) = 0.65\left(\frac{e_a(t)}{T_a(t)+273.15}\right)^{0.14} \tag{80}$$

And f (-) is a cloudiness factor (Jensen, Wright and Pratt, 1971; Wright and Jensen, 1972; Wright, 1982; Shuttleworth, 1992; Allen *et al.*, 1998)

$$f(t) = 1.35\frac{K_d(t)}{K_{d0}(DOY)} - 0.35 \tag{81}$$

with DOY [-] the numeric day of the year

With K_d [MJ/m²/day] downward shortwave radiation, and K_{d0} [MJ/m²/day] downward shortwave radiation for a clear sky, given as (Liu and Jordan, 1960; Dong *et al.*, 1992; Donohue, Mcvicar and Roderick, 2009):

$$K_{d0}(DOY) = \tau_0 R_a(DOY) \tag{82}$$

where R_a (MJ/m^2/day) is extraterrestrial radiation, and the atmospheric transmissivity for a clear sky τ_0 (-) for the southern hemisphere is (Roderick, 1999)

$$\tau_0 = 0.8 \tag{83}$$

while a value of 0.7-0.75 could be used for the northern hemisphere (Roderick, 1999).

The extraterrestrial radiation R_a [MJ/m^2/day] is given by (Liu and Jordan, 1960; Iqbal, 1983; Shuttleworth, 1992; Allen *et al.*, 1998; Duffie and Beckman, 2013)

$$R_a(DOY) =$$

$$\frac{24}{\pi} I_{SC} E_0(DOY)(\omega(DOY) \sin \phi \sin \delta(DOY) + \cos \phi \cos \delta (DOY) \sin \omega(DOY)) \tag{84}$$

where I_{SC} [kJ/m^2/h] is the solar constant (4921 kJ/m^2/h or 1367 W/m^2) (Fröhlich and Brusa, 1981; Iqbal, 1983) and E_0 (-) is the eccentricity correction factor of the Earth's orbit (around the sun) (Iqbal, 1983; Allen *et al.*, 1998; Duffie and Beckman, 2013)

$$E_0(DOY) = 1 + 0.033 \cos\left(\frac{2\pi DOY}{365}\right) \tag{85}$$

Substituting the values for the atmospheric transmissivity for a clear sky τ_0 (-) and the solar constant I_{SC} [kJ/m^2/h] gives

$$K_{d0}(DOY) = \frac{94.5}{\pi} E_0(DOY)(\omega(DOY) \sin \delta(DOY) \sin \phi + \cos \delta (DOY) \cos \phi \sin \omega(DOY)) \tag{86}$$

where $\boldsymbol{\omega}$ [radians] is sunset hour (Liu and Jordan, 1960; Iqbal, 1983; Shuttleworth, 1992; Allen *et al.*, 1998), given by

$$\omega(DOY) = \cos^{-1}(-\tan \phi \tan \delta(DOY)) \tag{87}$$

with $\boldsymbol{\phi}$ [radians] latitude, and δ (radians) solar declination calculated as (Spencer, 1971; Iqbal, 1983)

$$\delta(DOY) = 0.006918 - 0.39912 \cos \Gamma(DOY) + 0.070257 \sin \Gamma(DOY) - 0.006758 \cos 2\Gamma(DOY) + 0.000907 \sin 2\Gamma(DOY) - 0.002697 \cos 3\Gamma(DOY) + 0.00148 \sin 3\Gamma(DOY) \tag{88}$$

where Γ [radians] is the day angle, given by Iqbal (1983) as

$$\Gamma(DOY) = 2\pi \frac{(DOY-1)}{365} \tag{89}$$

The day length N [h] can be calculated from the sunset hour $\boldsymbol{\omega}$ (radians) as (Iqbal, 1983; Shuttleworth, 1992; Duffie and Beckman, 2013)

$$N(DOY) = 2\omega(DOY)\frac{24}{2\pi} \tag{90}$$

From which the daily fraction of daylight hours f_{day} [-] is computed

$$f_{day}(DOY) = \frac{N(DOY)}{24} \tag{91}$$

Therefore the net outgoing longwave radiation $R_{ln\,out}$ is

$$R_{ln\,out}(t) = \sigma(T_a(t) + 273.15)^4 \left(1 - 0.65 \left(\frac{e_a(t)}{T_a(t)+273.15}\right)^{0.14}\right) \left(1.35 \frac{K_d(t)}{K_{do}(DOY)} - 0.35\right) \quad (92)$$

Which is similar to the net outgoing longwave radiation of Allen et al. (1998), but with different parameterisations for the atmospheric emissivity for a clear sky and daytime air temperature (and downward shortwave radiation for a clear sky).

Finally the downward longwave radiation L_d [W/m²] can be represented as:

$$L_d(t) = \sigma(T_a(t) + 273.15)^4 - f(t)\big(1 - \varepsilon_{a0}(t)\big)\sigma(T_a(t) + 273.15)^4 \quad (93)$$

or

$$L_d(t) = \sigma(T_a(t) + 273.15)^4\{1 - [1 - \varepsilon_{a0}(t)]f(t)\} \quad (94)$$

or after substitution

$$L_d(t) = \sigma(T_a(t) + 273.15)^4\left\{1 - \left[1 - 0.65\left(\frac{e_a(t)}{T_a(t)+273.15}\right)^{0.14}\right]\left(1.35\frac{\overline{K_d}(t)}{K_{do}(DOY)} - 0.35\right)\right\} \quad (95)$$

This is similar to the equation for L_d in Donohue et al. (2009), but with different parameterisations for the atmospheric emissivity and transmissivity for a clear sky.